

Earth's Future

RESEARCH ARTICLE

10.1029/2024EF005356

Key Points:

- Nitrogen deposition and extractable soil nitrogen decreased with elevation, while the microbial community was similar across elevation
- Net nitrogen transformation rates corresponded to the abundance of the nitrifier gene, *amoA*
- Future disturbances, such as wildfires, could alter the ability of the soils to process and retain current nitrogen deposition levels

Supporting Information:

Supporting Information may be found in the online version of this article.

Correspondence to:

D. A. Report,
darepert@usgs.gov

Citation:

Report, D. A., Heindel, R. C., Murphy, S. F., & Jeanis, K. M. (2025). Relationship of atmospheric nitrogen deposition to soil nitrogen cycling along an elevation gradient in the Colorado Front Range. *Earth's Future*, 13, e2024EF005356. <https://doi.org/10.1029/2024EF005356>

Received 17 SEP 2024

Accepted 12 DEC 2024

Author Contributions:

Conceptualization: Deborah A. Report, Ruth C. Heindel, Sheila F. Murphy
Data curation: Deborah A. Report, Sheila F. Murphy, Kaitlyn M. Jeanis
Formal analysis: Deborah A. Report, Sheila F. Murphy, Kaitlyn M. Jeanis
Funding acquisition: Sheila F. Murphy
Investigation: Deborah A. Report, Sheila F. Murphy
Methodology: Deborah A. Report, Sheila F. Murphy, Kaitlyn M. Jeanis
Project administration: Deborah A. Report, Sheila F. Murphy

Published 2025. This article is a U.S. Government work and is in the public domain in the USA. Earth's Future published by Wiley Periodicals LLC on behalf of American Geophysical Union. This is an open access article under the terms of the [Creative Commons Attribution License](#), which permits use, distribution and reproduction in any medium, provided the original work is properly cited.

Relationship of Atmospheric Nitrogen Deposition to Soil Nitrogen Cycling Along an Elevation Gradient in the Colorado Front Range

Deborah A. Report¹ , Ruth C. Heindel² , Sheila F. Murphy¹ , and Kaitlyn M. Jeanis¹

¹U.S. Geological Survey, Water Resources Mission Area, Boulder, CO, USA, ²Environmental Studies Department, Kenyon College, Gambier, OH, USA

Abstract Microbial processing of atmospheric nitrogen (N) deposition regulates the retention and mobilization of N in soils, with important implications for water quality. Understanding the links between N deposition, microbial communities, N transformations, and water quality is critical as N deposition shifts toward reduced N and remains persistently high in many regions. Here, we investigated these connections along an elevation transect in the Colorado Front Range. Although rates of N deposition and pools of extractable N increased down the elevation transect, soil microbial communities and N transformation rates did not follow clear elevational patterns. The subalpine microbial community was distinct, corresponding to a high C:N ratio and low pH, while the microbial communities at the lower elevation sites were all very similar. Net nitrification, mineralization, and nitrification potential rates were highest at the Plains (1,700 m) and Montane (2,527 m) sites, suggesting that these ecosystems mobilize N. In contrast, the net immobilization of N observed at the Foothills (1,978 m) and Subalpine (3,015 m) sites suggests that these ecosystems retain N deposition. The contrast in N transformation rates between the plains and foothills, both of which receive elevated N deposition, may be due to spatial heterogeneity not captured in this study and warrants further investigation. Stream N concentrations from the subalpine to the foothills were consistently low, indicating that these soils are currently able to process and retain N deposition, but this may be disrupted if drought, wildfire, or land-use change alter the ability of the soils to retain N.

Plain Language Summary Deposition of nitrogen (N) from the atmosphere can have important implications for water quality and ecosystems. The amount and relative contribution of atmospheric nitrate (NO_3^-) and ammonium (NH_4^+) deposition can vary substantially along elevation gradients, influenced by proximity to urban and agricultural sources and prevailing wind patterns. The structure and function of the microbial community, soil composition, and precipitation patterns along these gradients are important factors in how this N is transformed and transported and can ultimately affect water quality. For this study, we measured atmospheric NO_3^- and NH_4^+ deposition, soil microbial community composition, N transformation rates, soil carbon (C) and N content, and stream nutrient concentrations seasonally at several sites across a 1,400-m elevation gradient in the Colorado Front Range. Results of our study showed that while sites in closer proximity to urban and agricultural atmospheric N sources received greater atmospheric deposition of inorganic nitrogen, processing of this nitrogen in the soils varied considerably. This suggests that a site's capacity to retain or lose N depends on certain soil characteristics as well as the ability of the local microbial community to utilize N.

1. Introduction

Across the United States (U.S.), the quantity and form of reactive nitrogen (N) deposited from the atmosphere have shifted over the past three decades due to regulations and land use change (Li et al., 2016). While emissions and deposition of oxidized N (NO_x) have significantly diminished due to the Clean Air Act Amendment of 1990 (Benish et al., 2022; Likens et al., 2021), emissions and deposition of reduced N (NH_3 and NH_4^+) remain unregulated and have either not declined or increased in some regions of the country (Benish et al., 2022; Driscoll et al., 2024; Fenn et al., 2018; Li et al., 2016). Vehicles, agricultural activities, and biomass burning all contribute to ammonia emissions (Felix et al., 2023; Fenn et al., 2018; Lindaas et al., 2021), making it likely that reduced N deposition will remain elevated due to ongoing urban development, agricultural intensification, and increasing wildfire activity. The resulting shift toward reduced N in atmospheric deposition (Benish et al., 2022; Du et al., 2014) has implications for air quality, ecosystem biodiversity and productivity, and water quality. Although

Resources: Deborah A. Repert, Sheila F. Murphy, Kaitlyn M. Jeanis

Software: Deborah A. Repert, Kaitlyn M. Jeanis

Supervision: Deborah A. Repert, Sheila F. Murphy

Validation: Deborah A. Repert, Sheila F. Murphy, Kaitlyn M. Jeanis

Visualization: Deborah A. Repert, Ruth C. Heindel, Sheila F. Murphy, Kaitlyn M. Jeanis

Writing – original draft: Deborah A. Repert, Ruth C. Heindel, Sheila F. Murphy, Kaitlyn M. Jeanis

Writing – review & editing: Deborah A. Repert, Ruth C. Heindel, Sheila F. Murphy

the long-term changes to atmospheric N deposition are well-documented and relatively straightforward, the connections between changing N deposition and water quality are often challenging to untangle (Lassiter et al., 2023; Lin et al., 2024), due to the many processes that can alter N once it is deposited on a terrestrial environment and before it enters a water body.

Microorganisms within the soil play a pivotal role in processing N from atmospheric deposition, ultimately influencing soil nutrient cycling and overall productivity (Fierer et al., 2012; Fog, 1988; Freedman et al., 2015; Zhang et al., 2018). Ammonium (NH_4^+) and nitrate (NO_3^-) are typically the forms of N deposited from the atmosphere and undergo various microbial-facilitated processes in the soil that affect their transformation, mobility, and availability for plant growth (Booth et al., 2005; Li et al., 2019). Nitrification is an important microbial process in soils that converts NH_4^+ to NO_3^- . It is characteristically facilitated by ammonia-oxidizing archaea and bacteria (AOA and AOB), such as *Nitrososphaera* and *Nitrosomonas*, and nitrite-oxidizing bacteria (NOB), such as *Nitrobacter*, although some species of *Nitrospira* are capable of complete ammonia oxidation to nitrate (Daims et al., 2015; Van Kessel et al., 2015). Nitrification increases the availability of NO_3^- for plant uptake but can also lead to N loss through leaching and runoff.

In addition, soil microbes mediate the immobilization of N via incorporation into microbial biomass and soil organic matter, thereby regulating N availability and nutrient cycling dynamics. Soil microbial community composition and activity can vary spatially and temporally as environmental conditions, such as soil moisture, temperature, pH, and nutrient availability shift. Altered nutrient availability due to N deposition can thus shape the soil microbial community (Bowman et al., 2018; Fierer et al., 2012; Zhang et al., 2018); chronic N application experiments have been shown to not only alter the composition of the active microbial community but also reduce the activity of key enzymes that degrade plant material (Carreiro et al., 2000; Freedman et al., 2015). Fierer et al. (2012) observed a shift from oligotrophic to copiotrophic microbial community composition in soils with high N amendment ($>270 \text{ kg N ha}^{-1} \text{ yr}^{-1}$). This variability in microbial community affects the rates and efficiency of N processing in terrestrial ecosystems, as different microbial species exhibit varying preferences and efficiencies in N transformations (Crowther et al., 2019; Li et al., 2021; Philpott et al., 2013).

The Colorado Front Range, U.S., extending from the Boulder-Denver metro area in the east to the Continental Divide in the west across variable vegetation, soil type and bedrock, is an ideal location to study the dynamics of N deposition and soil N processing. The Colorado Front Range experiences opposing gradients of precipitation and ammonia emissions, with the highest precipitation in the alpine and subalpine zones, and the highest ammonia emissions from urban and agricultural activities on the plains (Felix et al., 2023). These opposing gradients result in elevated N deposition of $\sim 4.5 \text{ kg N ha}^{-1} \text{ yr}^{-1}$ in the urban and foothill ecosystems, and lower, yet still elevated, deposition of $\sim 2.5 \text{ kg N ha}^{-1} \text{ yr}^{-1}$ in the montane and subalpine ecosystems (Heindel et al., 2022; Wetherbee et al., 2019). At the lower elevations, N deposition is strongly dominated by reduced N (72%), while at the higher elevations, reduced and oxidized forms of N are more equivalent (58% reduced; Heindel et al., 2022). In addition to the elevation gradient in N deposition, there is also extreme seasonal variability in N deposition, with the greatest N deposition in the spring when ammonia emissions from vehicles, biomass burning, and agriculture coincide with high precipitation (Felix et al., 2023; Heindel et al., 2022). With the growing population in the Boulder-Denver metro area as well as a likely increase in N deposition due to the intensification of wildfires (Westerling et al., 2006), it is likely that N deposition in this region, dominated by reduced forms of N, will remain constant or increase in the future.

The Colorado Front Range has also been a region of active research into soil N cycling, especially at the Niwot Ridge long-term ecological research site (e.g., Bowman et al., 2018; Lieb et al., 2011). In the alpine zone, there is high spatial variability in rates of soil N processing across different ecosystem types, and soil moisture, temperature, and carbon-to-nitrogen (C:N) ratios are key controls (Chen et al., 2020). In addition, long-term N application experiments have demonstrated the sensitivity of the soil microbial communities to elevated N availability, with oligotrophic taxa such as Acidobacteriota and Verrucomicrobiota decreasing in abundance with increasing N addition (Brigham et al., 2022). Although positive net N mineralization rates are typically measured in the alpine zone, contributing NO_3^- to surface waters (Clark et al., 2021), microbial immobilization of N has been measured during the growing season in the subalpine forests (Chen et al., 2020). In the montane forests, the retention and transport of N differs between North-facing and South-facing slopes, with much less microbial uptake of N on the drier South-facing slopes (Hinckley et al., 2014). Finally, in the lower elevation plains directly adjacent to Boulder, accelerated soil N cycling has been linked to the presence of the invasive tall oatgrass

(*Arrhenatherum elatius* subsp. *elatius*), although this connection is dependent on both site and season (Hinckley et al., 2022). While this large body of previous research suggests that soil N cycling differs by elevation in the Colorado Front Range, few studies have measured soil N processing across an elevation transect, while simultaneously quantifying atmospheric N deposition.

In this study, we investigated how soils along an elevation transect from the low-elevation plains to the subalpine zone of the Colorado Front Range differ in their ability to process N. We hypothesized that the microbial communities at different elevations would be distinct, due to differences in soil properties and rates of N deposition. Due to these different microbial communities, we also hypothesized that rates of soil N transformations would differ across the elevation transect, with faster rates of soil N transformations at the lower elevation ecosystems where N deposition is greatest. In addition, we sampled water quality of small watersheds across the elevation gradient to assess whether differences in N deposition and soil N cycling affected instream N concentrations. Results from this study will help predict the ecosystem consequences of continued N deposition across the Colorado Front Range.

2. Materials and Methods

2.1. Study Site

This study was conducted along an elevational gradient in the Boulder Creek Watershed, in the Colorado Front Range (Figure 1). The watershed ranges in elevation from 1,480 to 4,120 m and can be divided into five major climatic zones/ecoregions: Plains (1,450–1,800 m), Foothills (1,800–2,400 m), Montane (2,400–2,700 m), Subalpine (2,700–3,500 m), and Alpine (3,500–4,120 m) (Figure 1; Murphy, 2006). Mean annual precipitation is 400–600 mm in the plains, foothills, and montane zones, and increases with elevation in the subalpine and alpine regions to 1,100 mm near the Continental Divide (Murphy, 2006; Murphy et al., 2015). The plains region is primarily underlain by sedimentary rock and alluvium, while the higher elevations are primarily underlain by metamorphic and granitic bedrock (Figure 1). Land cover in the foothills through alpine regions is mostly forest, with areas of shrub/scrub and herbaceous land cover, while land cover in the plains region is primarily developed and herbaceous (Figure S1 in Supporting Information S1, Table 1, Table S1 in Supporting Information S1). The Plains East site (CO85) was located within the city of Boulder adjacent to parking lots, a highly trafficked road, and active construction (Heindel et al., 2022), and thus represented an area highly affected by urbanization (Figure 1); due to the lack of undisturbed ground, no soil samples were collected. Soil samples were instead collected from the Plains West site (FP), located immediately west of the urban boundary of the city of Boulder on grassland that has been preserved as open space.

2.2. Atmospheric N Deposition

Atmospheric N deposition was measured at sites in the plains, foothills, montane, and subalpine regions. We evaluated wet deposition N data from the National Atmospheric Deposition Program National Trends Network (NADP-NTN) sites CO84, CO85, CO94, and CO90 (Figure 1, Table 1; National Atmospheric Deposition Program, 2022; Wetherbee et al., 2019; Wetherbee et al., 2021). Ion exchange resin (IER) columns were co-located with samplers deployed by the NADP-NTN at sites CO84, CO85, CO94, and CO90, and were installed at one additional site in the plains region (Plains W/FP) (Figure 1, Table 1; National Atmospheric Deposition Program, 2022; Wetherbee et al., 2019; Wetherbee et al., 2021). The IERs, which collected wet and dry deposition, were deployed for 2–3-month intervals during the snow-free months in spring, summer, and fall of 2018 and 2019. Samples were collected at the Plains E, Foothills, and Montane sites for all intervals during the study period, at the Plains W site in May–June (MJ) and July–September (JAS) 2018, and at the Subalpine site in May–June (MJ), July–August (JA), and September–October (SO) 2019. IERs were extracted with 2 molar (M) potassium chloride (KCl), and the resultant extracts were analyzed for NH_4^+ and nitrate plus nitrite ($\text{NO}_3^- + \text{NO}_2^-$). Due to incompatibility of the IER columns during winter conditions, from Jan–Apr 2019 it was necessary to utilize nitrogen data collected from NADP-NTN collectors for statistical analyses during that 4 month period. In the study by Heindel et al. (2022), nitrogen deposition results from the IER collectors were shown to relate well to results from NADP-NTN collectors. Detailed site information and IER methods are described in Heindel et al. (2022) and Repert et al. (2021).

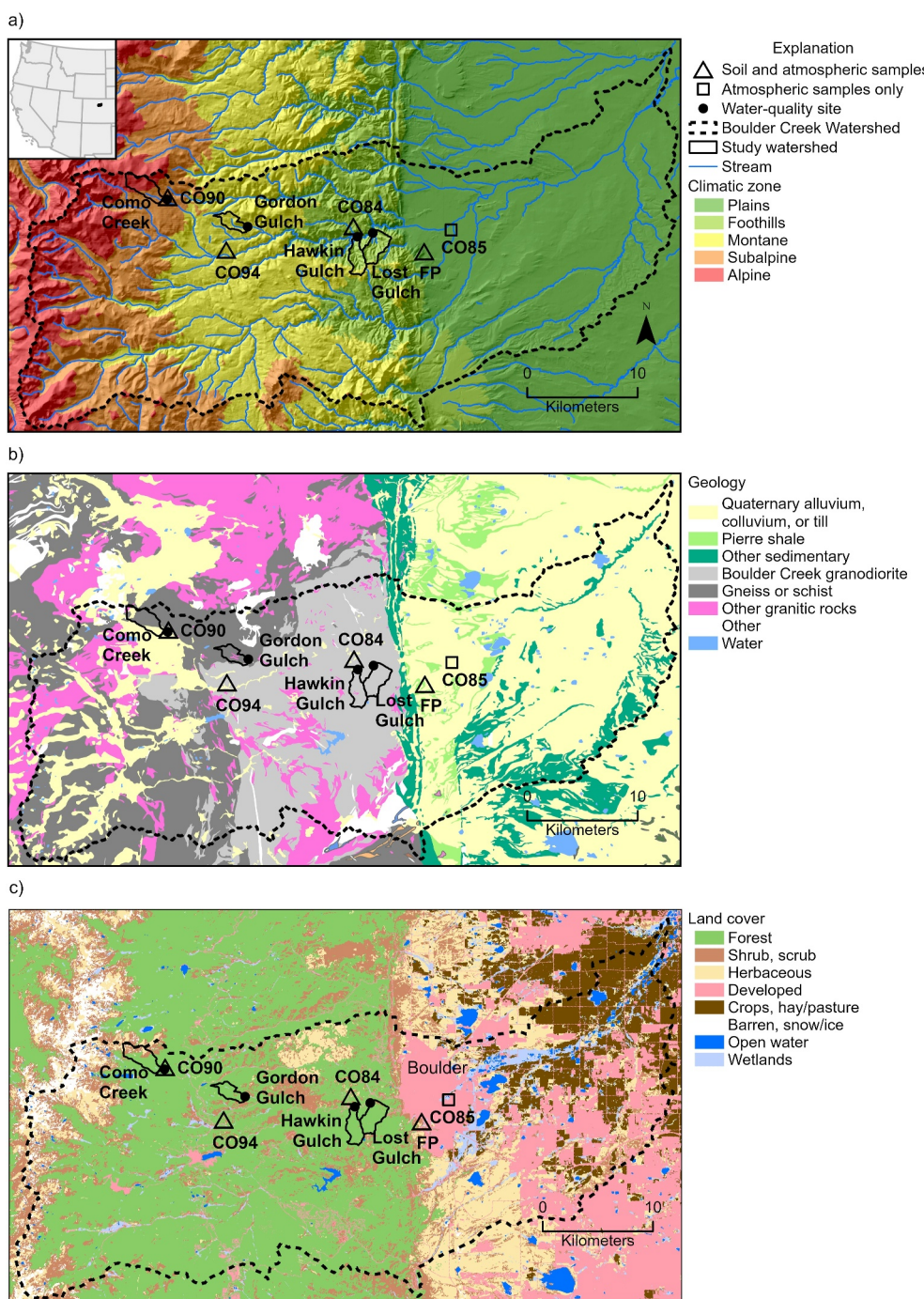


Figure 1. Maps of Boulder Creek Watershed, Colorado and study sites showing (a) climatic zones (adapted from Murphy, 2006); (b) geology (Cole & Braddock, 2009; Kellogg et al., 2008); and (c) 2019 land cover (Dewitz & U.S. Geological Survey, 2021).

2.3. Soil Collection, Processing, and Characterization

Soil samples were collected five times from October 2018 to October 2019 at the Montane, Foothills, and Plains W sites adjacent to where IER assemblies were deployed. Soil samples were collected once, in August 2019, at the Subalpine site (Table 1). Soil cores from the top 0–10 cm were collected at each site, composited, sieved to <2-mm size fraction, and the coarse size fraction discarded. Soil subsamples were characterized at all sites for percent moisture content, C and N content, and pH. Soil plant available N was determined using a combination of

Table 1*Detailed Site Information and Sample Types, Locations, and Collection Times for This Study*

| Ecosystem | Plains East (E) | Plains West (W) | Foothills | Montane | Subalpine |
|---|--|--|--|--|--|
| Atmospheric and soil samples | | | | | |
| Site | CO85 | FP | CO84 | CO94 | CO90 |
| Elevation (m) | 1600 | 1700 | 1978 | 2527 | 3015 |
| Surface geology ^a | Alluvium | Shale | Granodiorite | Granodiorite | Glacial till |
| Land cover ^b | Developed | Grassland | Grassland | Forest | Forest |
| Dates of IER installations | April–June 2018 June–September 2018 October–November 2018 May–July 2019 July–September 2019 September–November 2019 | April–June 2018 June–September 2018 | April–June 2018 June–September 2018 | April–June 2018 June–September 2018 | — — — May–July 2019 July–September 2019 September–November 2019 |
| Dates NADP data used ^c | January–April 2019 | — | January–April 2019 | January–April 2019 | — |
| Dates of soil collection | — — — — — — | 9 October 2018 8 February 2019 13 May 2019 5 August 2019 20 October 2019 | 9 October 2018 8 February 2019 13 May 2019 5 August 2019 20 October 2019 | 9 October 2018 8 February 2019 13 May 2019 5 August 2019 20 October 2019 | 9 October 2018 8 February 2019 13 May 2019 5 August 2019 20 October 2019 |
| Water quality samples | | | | | |
| Ecosystem | | Foothills | Foothills | Montane | Subalpine/Alpine |
| Watershed | | Lost Gulch | Hawkin Gulch | Gordon Gulch | Como Creek |
| Elevation at sampling site (m) | | 1766 | 1829 | 2435 | 3018 |
| Drainage area (km ²) ^d | | 4.45 | 3.55 | 2.69 | 4.82 |
| Mean annual precipitation (mm) ^d | | 534 | 541 | 511 | 892 |
| Dominant geology ^a | | Granodiorite | Granodiorite | Gneiss or schist | Gneiss or schist, glacial till |
| % Forest ^b | | 94.0 | 98.8 | 94.0 | 58.8 |
| Dates of water-quality sampling | | 8 April 2019, 20 May 2019–2 August 2019 ^e | 8 April 2019, 30 May 2019–13 August 2019 ^e | 30 May 2019–30 August 2019 | 12 June 2019–30 August 2019 |
| Number of samples | | 9 | 10 | 10 | 8 |

Note. Atmospheric and soil samples. IER, Ion-exchange resin; NADP, National Atmospheric Deposition Program. ^aGeology: Cole & Braddock (2009); Kellogg et al. (2008). ^bLand cover and percent forest (2019): Dewitz and U.S. Geological Survey (2021). ^cIER data not collected due to winter conditions, NADP data used instead. ^dDrainage area and mean annual precipitation (1971–2000): U.S. Geological Survey (2019). ^eSampling ended when stream channel went dry.

deionized water and KCl extraction methods. KCl is a more efficient extractant of NH_4^+ and NO_3^- from soils (Li et al., 2012) but can negatively impact NO_2^- by conversion to gaseous N (Homyak et al., 2015). To determine whether measurable NO_2^- was available in the soils the deionized water extraction method was employed in addition to the KCl extraction method. This method also allowed for the analysis of total dissolved nitrogen (TDN) and an estimate of organic nitrogen (OrgN) by difference. Soil bulk density was determined at the Foothills and Montane sites, but not the Plains W and Subalpine sites due to access issues at the time of sampling. Further details of the methods used can be found in Repert et al. (2023).

2.4. N-Cycling Processes

Net nitrification, net N mineralization, and nitrification potential rates were determined at each site following the methods of Hart et al. (1994). Further details are described in Repert et al. (2023). Briefly, net nitrification and N mineralization rates were determined by adding <2-mm sieved, field-moist soil to 100-mL amber glass jars and incubating undisturbed at room temperature. Duplicate jars were processed after approximately 0, 1, 2, and 3 weeks by extracting with 2 M KCl. Samples were preserved and analyzed for $\text{NO}_3^- + \text{NO}_2^-$ and NH_4^+ concentrations. Net nitrification rates were determined by measuring the change in concentration of $\text{NO}_3^- + \text{NO}_2^-$ from the first collection timepoint (T_0) to the last collection timepoint (T_f) and net N mineralization by measuring the change in concentration of $\text{NO}_3^- + \text{NO}_2^-$ and NH_4^+ from T_0 to T_f . Nitrification potential rates were determined by combining 15 grams (g) of <2 mm sieved, field moist soil with 100 mL of a 1.5 mM $(\text{NH}_4)_3\text{PO}_4$ solution, adjusted to pH 6.6, in triplicate 125 mL Erlenmeyer flasks. The flasks were mixed at room temperature on an orbital shaker and 5 mL subsamples removed from two of the three flasks after ~2, 6, 18, 24, 30, 43, 51, 68 hr, then filtered and preserved for $\text{NO}_3^- + \text{NO}_2^-$ analysis. The third replicate flask was used to measure pH at each timepoint. At the final timepoint the remaining sample was filtered and preserved for $\text{NO}_3^- + \text{NO}_2^-$, NH_4^+ , TDN, and dissolved organic carbon (DOC) analysis. Nitrification potential rates were determined by measuring the $\text{NO}_3^- + \text{NO}_2^-$ concentration change over time (Repert et al., 2023).

2.5. Molecular Characterization

DNA was extracted from soil using the DNeasy PowerSoil kit (Qiagen, Inc., Germantown, MD, document #HB-2266-002) and quantified using Promega™ QuantiFluor® dsDNA Dye System (Promega, Madison, WI) on a Denovix DS-11 Fluorometer (Denovix, Wilmington, DE). Extracted environmental DNA (eDNA) was stored at -20°C until downstream analysis. Prior to sending to Michigan State University (MSU) Research Technology Support Facility (RTSF) for Next-Generation Sequencing, extracted samples were normalized to a concentration of approximately 1 nanogram per microliter ($\text{ng } \mu\text{L}^{-1}$) by diluting with high grade molecular water. At MSU RTSF, Illumina amplicon libraries, iTags (Illumina, Inc., San Diego, CA), were generated by amplification of the V4 hypervariable region of bacterial and archeal 16S rRNA gene using dual indexed, Illumina compatible primers (515f/806r) (Caporaso et al., 2011) and sequenced following a standard protocol (Kozich et al., 2013). Demultiplexed reads in FastQ format were paired and processed using QIIME 2™ version 2020.8 (Bolyen et al., 2019) at the USGS Advanced Research Computing (ARC) Yeti facility. Demultiplexed paired-end sequences were imported into QIIME 2™ (qiime tools import) then joined and denoised using Dada2 (qiime dada2 denoise-paired) to resolve nucleotide level differences between amplicon sequence variants (ASVs) (Callahan et al., 2016). ASVs were aligned using the MAFFT program (Katoh et al., 2002) and a phylogenetic tree was generated using FastTree (Price et al., 2010) from the masked alignment. ASVs were assigned taxonomy using the feature classifier plugin (Bokulich et al., 2018) with the classify-sklearn naïve Bayes taxonomy classifier method (qiime feature-classifier classify-sklearn) against Silva 99% reference sequences (Silva NR 138.1) (Pruesse et al., 2007; Quast et al., 2012; Robeson et al., 2021; Rognes et al., 2016). Beta diversity metrics (weighted UniFrac, Lozupone et al., 2007), and Principal Coordinate Analysis (PCoA) were performed with samples rarefied to 26,281 sequences per sample (qiime diversity core-metrics-phylogenetic).

Quantification for the gene encoding the active-site polypeptide of ammonia monooxygenase (*amoA*) from Betaproteobacteria (Rothauwe et al., 1997) was performed by Real-time polymerase chain reaction (quantitative PCR, qPCR) on a CFX96 Touch Real-Time PCR Detection System (BioRad, Hercules, CA). Fluorescence data were acquired from the instrument using CFX Manager™ software (<https://www.bio-rad.com/en-us/sku/1845000-cfx-manager-software?ID=1845000>). Gene copy numbers were determined against a calibration curve of plasmid standards (10^3 – 10^8 copies) and then normalized to DNA sample volume (gene copy μL^{-1}). DNA concentrations in the soil (copy number g^{-1}) were determined by normalizing the total gene copy yield to the mass of dry soil used in each DNA extraction. Further details of primers used, and thermal cycling conditions can be found in Repert et al. (2023).

2.6. Water Quality

Stream discharge and water quality were monitored in four minimally disturbed watersheds near the atmospheric and soil sample locations: Como Creek, which spans the subalpine and alpine region; Gordon Gulch, in the montane region; and Hawkin and Lost Gulches, which primarily drain the foothills region (Figure 1; Table 1).

Como Creek and Gordon Gulch are described in Williams et al. (2011), and Hawkin and Lost Gulches are described in Bukoski et al. (2021). Small watersheds in the plains area of the study contain urban development which introduces other N sources that would obscure the atmospheric signal, and thus were not sampled. Stream discharge of Hawkin and Lost Gulches were measured using a flow meter (AquaCalc Pro, JBS Instruments, Columbus, OH, USA); discharge of Gordon Gulch was obtained from Hydroshare (<https://www.hydroshare.org/resource/c2384bd1743a4276a88a5110b1964ce0/>); and discharge of Como Creek was obtained from NEON (<https://www.neonscience.org/field-sites/como>). Between 8 and 10 water-quality samples were collected as grab samples at the sites between April 2019 and August 2019 (Table 1). Water sampling methods followed standard techniques of filtering and preserving samples for laboratory analysis (Bukoski et al., 2021; McCleskey et al., 2012; Repert et al., 2024).

2.7. Analytical Methods

Water quality samples and deionized water extractions of soil samples were analyzed for major anion and cation concentrations using a Dionex Model ICS-5000 ion chromatograph (Smith et al., 2019), TDN concentration using a Skalar Formacs^{TN} Total Nitrogen analyzer equipped with an ND25 Total Nitrogen detector (Repert et al., 2014), and DOC concentrations by persulfate/UV oxidation using a Teledyne Tekmar Fusion TOC analyzer or an Oceanographic Instruments Analytical TOC analyzer Model 700 (Potter & Wimsatt, 2005 (EPA 415.3)). KCl-extracted soil samples were analyzed for $\text{NO}_3^- + \text{NO}_2^-$ and NH_4^+ concentrations by colorimetric detection using a SEAL Analytical AQ300 discrete analyzer. Total C and N content of the soil was determined by combustion at 980°C using an Exeter CE440 Elemental Analyzer (Smith et al., 2013). Ion exchange resin column KCl extracts were analyzed for $\text{NO}_3^- + \text{NO}_2^-$ and NO_2^- only concentrations using a Sievers Model 280i Nitric Oxide Analyzer with chemiluminescent detection (Garside, 1982) and for NH_4^+ concentration by colorimetric spectrophotometry using the indophenol blue method (Scheiner, 1976). Additional method details are available in Repert et al. (2021, 2023, 2024) as well as Text S1 in Supporting Information S1.

Statistical analyses were performed in XLSTAT (<https://www.xlstat.com/en/>) to determine relationships between environmental variables, using Pearson's correlation, and to determine significant differences between sites, using the Kruskal-Wallis non-parametric test. PCoA and Redundancy analysis (RDA) were determined using R version 4.1.0 with the package *psych* (Revelle, 2024) to investigate correlations among predictors and the package *vegan* (Oksanen et al., 2024) using family-level taxa with 2% relative abundance or greater (R Core Team, 2024).

3. Results

3.1. Atmospheric N Deposition Using Ion Exchange Resin (IER) Columns

Atmospheric deposition of total inorganic nitrogen (TIN) followed the expected pattern with elevation, with more TIN deposited at the lower elevations adjacent to urban and agricultural emissions (Figure 2) (Heindel et al., 2022). However, this elevation gradient was seasonally dependent; it was most pronounced during the spring months (MJ), when total levels of TIN deposition were highest across all elevations. The elevation gradient was also evident during the fall months (SON), but total levels of TIN deposition were much lower. During the summer months (JAS), there was little difference in TIN deposition across the elevation gradient.

Across all elevations and seasons, TIN deposition was dominated by reduced forms of N, accounting for 55%–84% of total N deposition (Figure 2, Figure S2 in Supporting Information S1). The proportion of reduced to oxidized forms of N also varied by season, with the highest proportion of reduced N deposited during the spring months, especially at the lower elevation sites. In other words, the spatial and seasonal patterns in TIN deposition described above were driven by patterns in reduced N deposition; there was less spatial and seasonal variation in oxidized N deposition.

3.2. Soil Characteristics

Soil total C and N also followed a pattern with elevation, with % C, % N, and the C:N ratio decreasing from the low-elevation Plains W site to the Montane site (Table 2, Table S2 in Supporting Information S1). While the percent N was lowest at the Subalpine site (continuing the elevation gradient), the percent C was highest, resulting in a much higher C:N ratio for the subalpine site (33.2) compared to the other sites (12.6–11.9). The Subalpine site was also distinct in soil pH, with a much lower value (5.39) compared to the narrow range of average soil pH

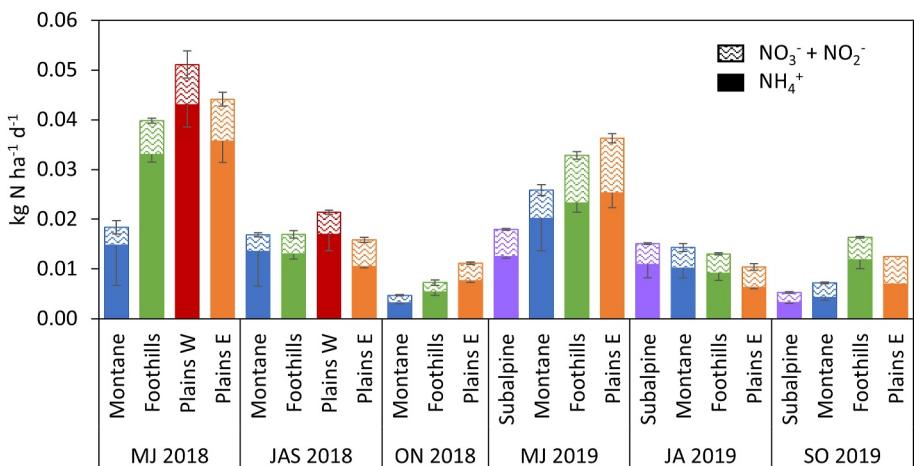


Figure 2. Seasonal deposition rates of ammonium (NH_4^+) and nitrate plus nitrite ($\text{NO}_3^- + \text{NO}_2^-$) at the Plains (E and W), Foothills, Montane, and Subalpine sites, in kilograms nitrogen per hectare per day ($\text{kg N ha}^{-1} \text{d}^{-1}$). Ion exchange resin (IER) columns were deployed for 2–3 month periods during the snow free months in 2018 and 2019, where MJ = May-June, JAS = July-September, ON = October-November, JA = July-August, and SO = September-October.

measured across the other elevations (6.57–6.76) (Table 2). Statistical analyses (Kruskal-Wallis pairwise comparisons) of the three primary sites (Plains W, Foothills, and Montane) showed soil % C and % N at the Plains W site was significantly ($p < 0.024$) higher than the Foothills and Montane sites, but the Foothills and Montane sites were not significantly different from one another. Soil C:N and pH were not significantly different between the 3 primary sites. Soil bulk densities measured at the Foothills and Montane sites were 1.46 and 1.35 g cm^{-3} , respectively, similar to values previously reported for montane sites in the Colorado Front Range (Hinckley et al., 2017).

In terms of the extractable nutrients, deionized water N extractions revealed an elevation gradient mirroring the soil total N pattern, with more total N extracted from soils from the lower elevation sites, with the exception of the ON 2018 season (Figure 3a). Oxidized inorganic N was higher in concentration than reduced inorganic N in deionized water extractions, with the exception of JA 2019 at the Subalpine, Foothills, and Plains sites. Reduced inorganic N was extracted more readily with KCl, with 2–5 times more reduced inorganic N measured in KCl extractions compared to the deionized water extractions (Figures 3a and 3b). Oxidized inorganic N concentrations were similar between the KCl and deionized water extractions.

Extractable DOC followed a pattern similar to the soil total C, with the most DOC extracted from soils at the Subalpine and Plains W sites, with the exception of the ON 2018 season (Figure 3c). In terms of seasonal variability, the Foothills and Plains W sites had the highest concentrations of DOC extracted in JA 2019, while the Montane site had the highest concentrations in ON 2018.

Table 2
Soil pH, Percent Carbon and Nitrogen, and Carbon to Nitrogen Ratio at the Study Locations From October 2018 to October 2019

| Ecosystem | pH ^a | Carbon ^b (%) | Nitrogen ^b (%) | C:N ^b | Soil bulk density ^c (g cm ⁻³) |
|-----------|-----------------|-------------------------|---------------------------|------------------|--|
| Plains W | 6.57 | 4.46 ± 0.84 | 0.35 ± 0.04 | 12.6 ± 0.88 | – |
| Foothills | 6.76 | 2.99 ± 0.37 | 0.25 ± 0.03 | 12.1 ± 1.03 | 1.46 |
| Montane | 6.67 | 2.46 ± 0.50 | 0.21 ± 0.05 | 11.9 ± 0.93 | 1.35 |
| Subalpine | 5.39 | 4.84 | 0.15 | 33.2 | – |

^aThe averages of the hydrogen ion concentrations were used for calculation of pH. ^bValues are averages and standard deviations of percent (%) carbon and nitrogen and carbon-to-nitrogen ratio (C:N). ^cSoil bulk density values are in grams per cubic centimeter (g cm⁻³).

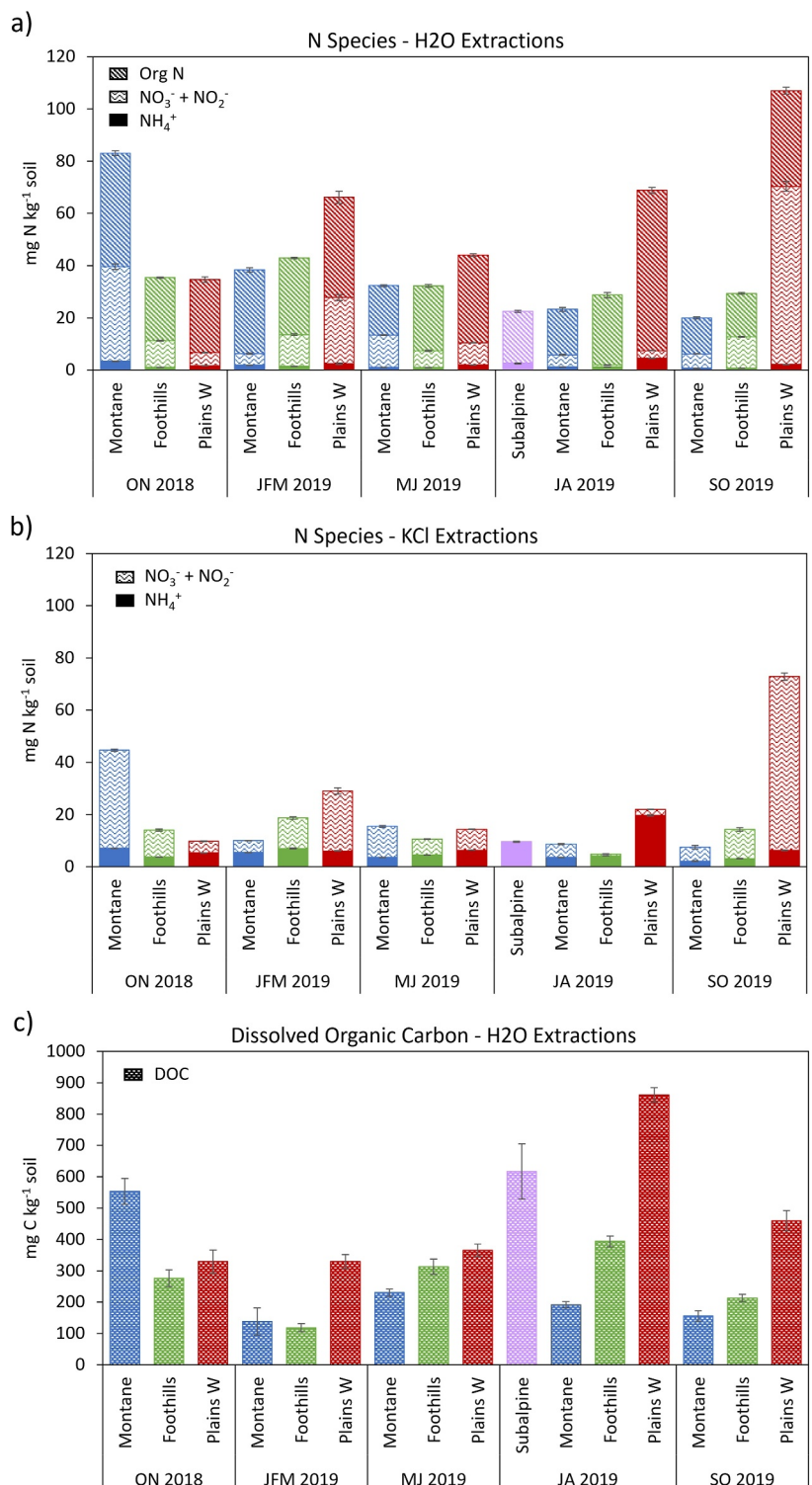


Figure 3. Deionized water (H₂O) and potassium chloride (KCl) extractions of <2 mm sieved air-dried soil collected from the Montane, Foothills, and Plains W sites from October–November (ON) 2018 to September–October (SO) 2019 and the Subalpine site in July–August (JA) only, showing (a) mass of ammonium (NH₄⁺), nitrate plus nitrite (NO₃⁻ + NO₂⁻), and organic N (Org N) extracted using deionized water, (b) mass of ammonium (NH₄⁺) and NO₃⁻ + NO₂⁻ extracted using KCl, and (c) mass of dissolved organic carbon (DOC) extracted using deionized water, as milligrams nitrogen or carbon per kilogram of dry weight soil (mg N or C kg⁻¹). For continuity of figures, date abbreviations correspond to dates of IER deployment rather than the date the soil was collected.

3.3. N-Cycling Processes

Net nitrification and N mineralization rates exhibited pronounced seasonal fluctuations across all sites. This was especially notable at the Foothills site, with near zero rates during the winter months of JFM 2019 and the summer in JA 2019, contrasting with positive rates during the fall of ON 2018, the spring of MJ 2019, and the fall of SO 2019 (Figures 4a and 4b). Soil net N mineralization rates were positive at the Plains W, Montane, and Subalpine sites (Figure 4b). The Subalpine site exhibited near-zero net nitrification rates in JA 2019 alongside significantly positive mineralization rates. The abundance of *amoA* (Figure 4a), the gene responsible for NH_4^+ oxidation, was significantly positively correlated with net nitrification and mineralization rates ($p < 0.0001$ and $p = 0.0003$, respectively) (Figure S3 and Table S3 in Supporting Information S1). While *amoA* abundance varied across sites, it was substantially higher at the Plains and Montane sites, coinciding with elevated net N mineralization rates, and lower at the Foothills and Subalpine sites, where nitrification and mineralization rates were comparatively diminished.

Throughout all seasons except SO 2019, nitrification potential rates were consistently greater at the Plains W site compared to the other sites (Figure 4c). Conversely, the Subalpine site exhibited negligible nitrification potential rates during JA 2019. There was less variability in nitrification potential rates (Figure 4c) across the sites compared to net nitrification (Figure 4a).

3.4. Taxonomy

Soil microbial community taxonomic composition showed minimal variability across sites or seasons, with the obvious exception of the Subalpine site (Figure 5). The soil communities were predominantly from the Actinobacteriota, Proteobacteria, Bacteroidota, Acidobacteriota, and Verrucomicrobiota phyla at the Montane, Foothills, and Plains sites. Within those phyla *Solirubrobacterales_67-14*, *Xanthobacteraceae*, *Chitinophagaceae*, *Vicinamibacterales_uncultured*, and *Chthoniobacteraceae* families dominated. Archaea and bacteria within the family *Nitrososphaeraceae* (aqua bars) in the phylum Crenarchaeota were evident at all sites, making up 0.3%–2.9% of the microbial community, but were a very minor component of the microbial community (<0.02%) at the Subalpine site. Microorganisms within this family are known ammonia oxidizers. The predominant families at the Subalpine site were found in the Proteobacteria and Acidobacteriota phyla, in particular *Xanthobacteraceae*, *Sphingomonadaceae*, *Acidobacteriales_uncultured*, and *Acidobacteriae_subgroup_2*.

Principal Coordinate Analysis (PCoA) of weighted UniFrac distances was used to compare differences in the microbial composition between the different sites and seasons (Lozupone & Knight, 2005) with 56.3% of the dissimilarities explained by the sum of the first (PC1) and second (PC2) principal coordinates (Figure 6). The microbial community was substantially different at the single Subalpine site collection (JA 2019) compared to the Montane, Foothills and Plains W sites collected during the 5 sampling times (Figure 6a). At the three primary sites, slight seasonal variations in microbial communities were observed, with the Plains site exhibiting the most pronounced shifts across seasons, while the Foothills site remained relatively stable (Figure 6b). The spring communities (MJ 2019) appeared to cluster together, as did the winter communities (JFM 2019).

Redundancy analysis (RDA) was used to identify the primary variables that explained the microbial community dissimilarity at the three primary sites, excluding the Subalpine site. Soil pH, % soil moisture, soil C:N, microbial biomass (ng DNA/gDW soil), atmospheric NH_4^+ deposition, KCl-extractable NH_4^+ , deionized water-extractable $\text{NO}_3^- + \text{NO}_2^-$, and 2-week antecedent precipitation were the most relevant environmental variables, explaining 51.4% of the variation in family-level (>2% maximum relative abundance) microbial composition ($p = 0.001$) (Figure 7). With the exception of the ON 2018 collection, the Plains W site was strongly positively correlated with extractable $\text{NO}_3^- + \text{NO}_2^-$ and NH_4^+ and negatively correlated with soil pH and microbial biomass. The Montane and Foothills sites were positively correlated with atmospheric NH_4^+ deposition and antecedent (cumulative 2-week prior) precipitation, and negatively correlated with % soil moisture (Figure 7).

3.5. Water Quality

Stream runoff and stream DOC concentrations showed a strong elevation gradient, while TDN and N species concentrations had no substantial difference with elevation (Figure 8, Table S4 in Supporting Information S1). Substantially higher runoff was measured in Como Creek, the subalpine/alpine watershed, due to it receiving about 70% more precipitation than the other watersheds (Table 1). DOC concentrations followed a similar

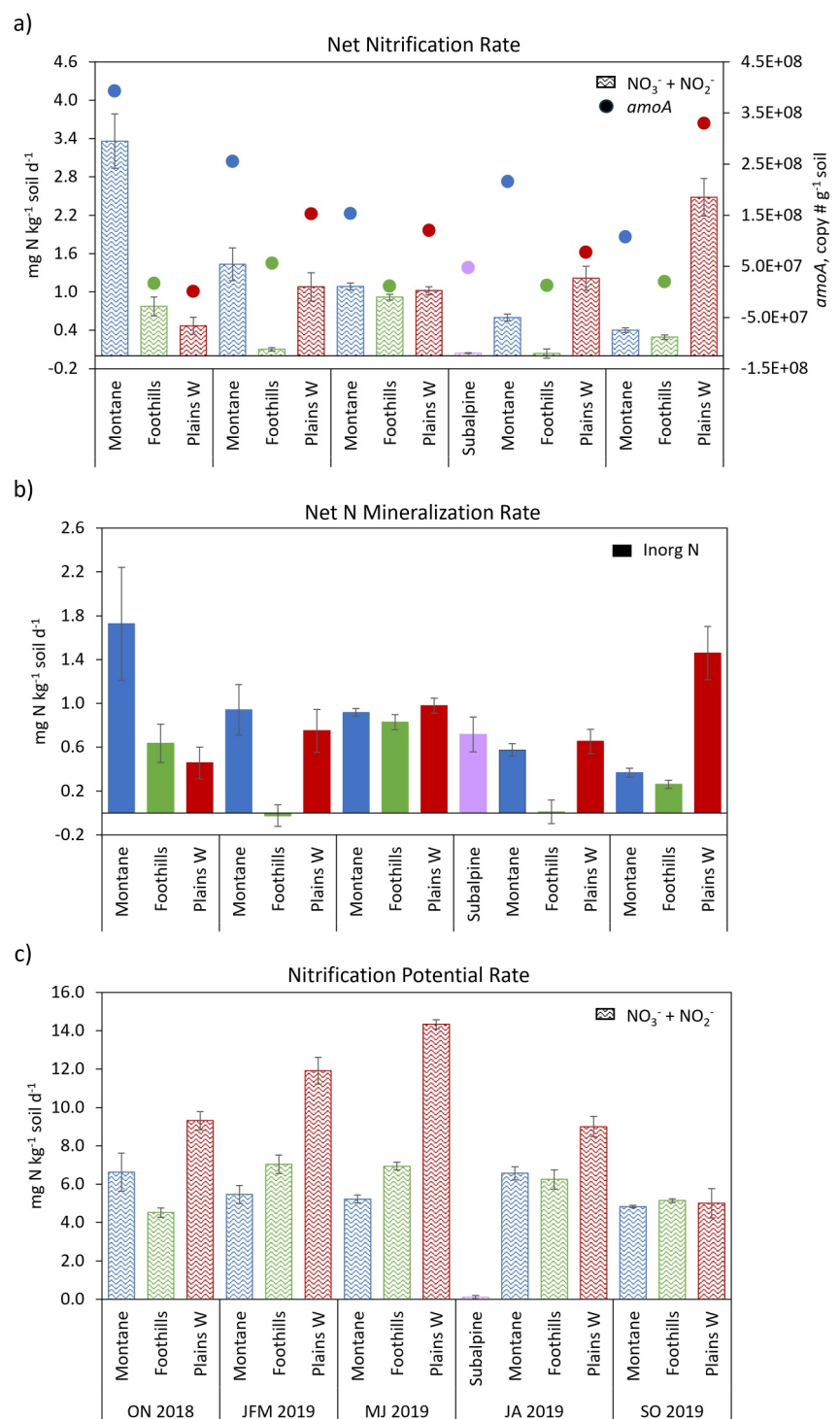


Figure 4. Net nitrogen transformation rates using field-moist, $<2\text{-mm}$ sieved soil and *amoA* gene abundance of starting soil material: (a) Net nitrification rates showing nitrate plus nitrite ($\text{NO}_3^- + \text{NO}_2^-$) concentration increase in milligrams (mg) of nitrogen (N) per kilogram (kg) of dry weight soil over time (d) and *amoA* gene abundance as copy number per gram (g) of dry weight soil over time, (b) net nitrogen mineralization rates showing change in $\text{NO}_3^- + \text{NO}_2^-$ plus ammonium (NH_4^+) concentrations in $\text{mg N kg}^{-1} \text{ d}^{-1}$, and (c) nitrification potential rates measured in soil plus water slurries containing an ammonium phosphate solution in $\text{mg N kg}^{-1} \text{ d}^{-1}$. Nitrification potential samples were collected several times over a 3-day period and analyzed for change in $\text{NO}_3^- + \text{NO}_2^-$ concentration with time. For continuity of figures, date abbreviations correspond to dates of IER deployment rather than the date the soil was collected.

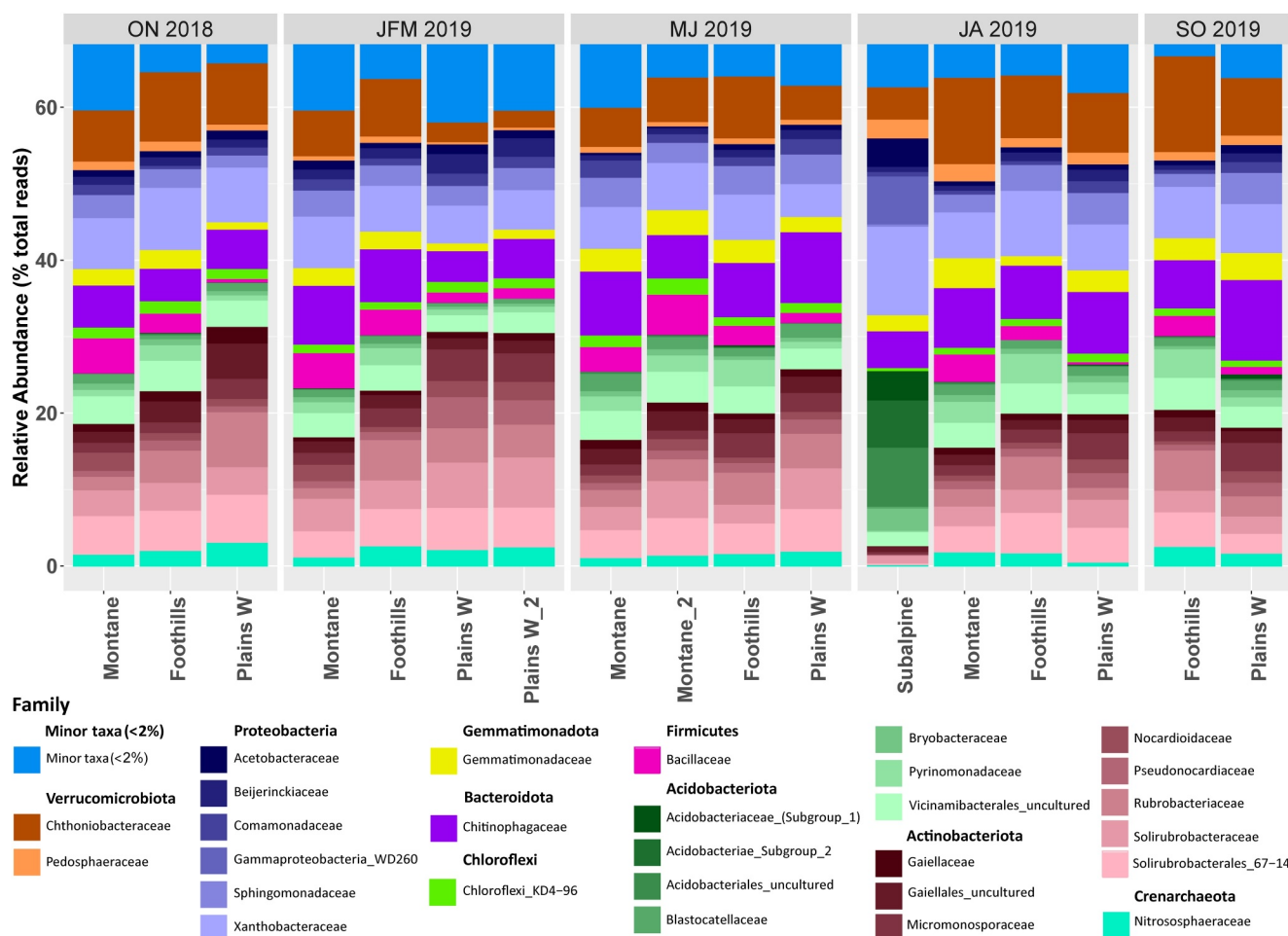


Figure 5. Stacked bar plot of the relative abundance of family-level taxonomy within the major phyla (in bold), with a >2 percent (%) maximum relative abundance using 16S rRNA sequencing from eDNA from <2-mm sieved soil samples collected seasonally at the Subalpine, Montane, Foothills, and Plains W sites.

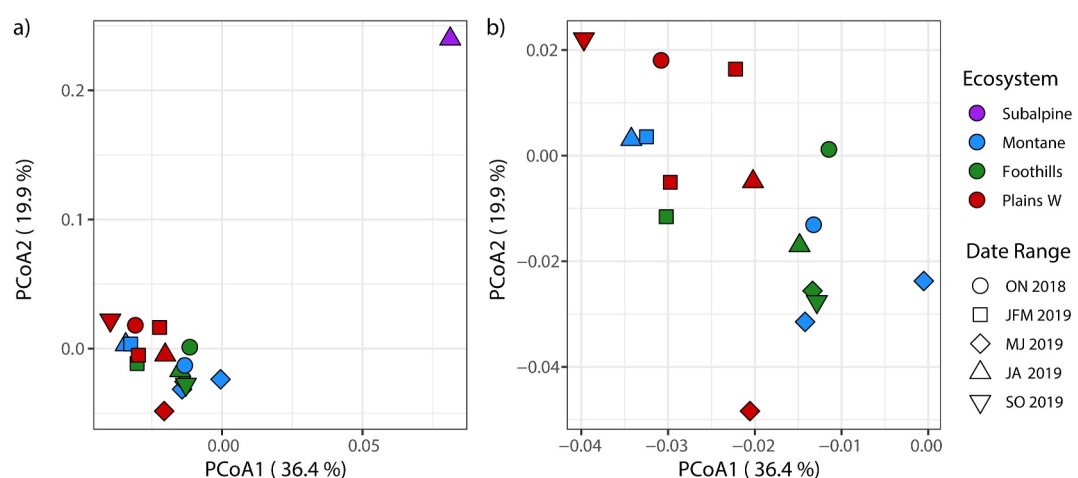


Figure 6. Principal Coordinate Analysis (PCoA) of the microbial community composition using weighted Unifrac distances. Sites are designated by color and season by shape. All sites are shown in panel (a), and a magnified view of the Montane, Foothills, and Plains W sites only are shown in panel (b).

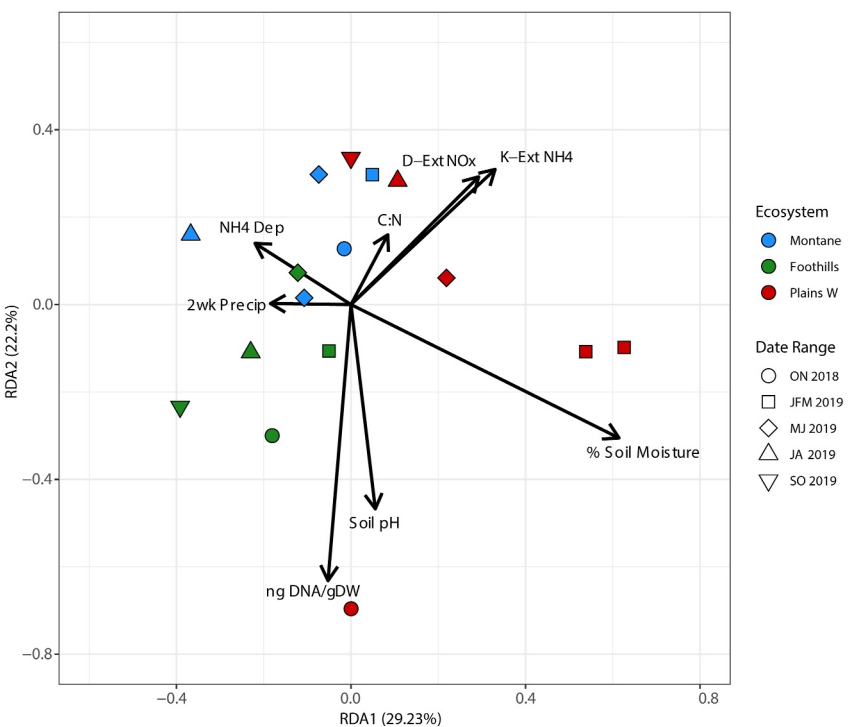


Figure 7. Redundancy analysis (RDA) showing the linear relationships between non-redundant environmental variables and components of microbial community variation, where C:N = carbon to nitrogen ratio, D-Ext NOx = deionized water extractable nitrate plus nitrite ($\text{NO}_3^- + \text{NO}_2^-$), K-Ext NH4 = KCl extractable ammonium, ng DNA/gDW = microbial biomass in nanograms of deoxyribonucleic acid per gram of dry weight soil, 2-week Precip = cumulative 2-week prior precipitation, and NH4 Dep = atmospheric ammonium deposition.

elevational trend; highest DOC concentrations were measured in Como Creek, with DOC concentrations ranging between 1.7 mg L^{-1} in August to 8.7 mg L^{-1} in June 2019 (this site was not accessible prior to June 2019). The two foothills sites, Lost and Hawkin Gulches, had the lowest stream discharge and DOC concentrations, with DOC concentrations ranging between 2.2 and 5.4 mg L^{-1} . Runoff and DOC concentrations were closely related at all sites ($r^2 0.727\text{--}0.976$, $p < 0.05$; Table S4 in Supporting Information S1) and both generally decreased over the summer as contributions from snowmelt decreased and flow paths shifted from near-surface to deeper flow paths (Boyer et al., 1997; Bukoski et al., 2021). Concentrations of N species were low at all sites. TDN concentrations were between 0.057 and 0.380 mg L^{-1} and showed no discernible trends across elevation; TDN was closely related to runoff at the montane and subalpine/alpine (GG and Como) watersheds ($r^2 0.710$ and 0.768 , $p < 0.05$), but not at the foothills watersheds (Figure 8). The majority of N was usually in the form of OrgN; NH_4^+ was usually below the detection limit (0.02 mg L^{-1}) and was always less than 0.06 mg L^{-1} . The Foothills site Hawkin Gulch had the highest NO_3^- concentrations, but usually the lowest OrgN concentrations (Figure 8).

4. Discussion

4.1. Spatial and Temporal Variability

As anticipated, atmospheric deposition and soil properties varied systematically along the steep elevation transect of the Colorado Front Range. As we have demonstrated in these results and in previous work (Heindel et al., 2022; Wetherbee et al., 2019), there was a clear gradient in atmospheric deposition with elevation. We observed higher rates of N deposition, especially in reduced forms, at the lower elevation sites closer to urban and agricultural sources. In the soils, concentrations of total N and extractable N also decreased with increasing elevation in tandem with atmospheric deposition. While we observed a similar pattern in total and extractable C for the Montane, Foothills, and Plains W sites (lower concentrations at the montane compared to the plains), the Subalpine site was distinct, with very high concentrations of total and extractable C. The high levels of soil C at the

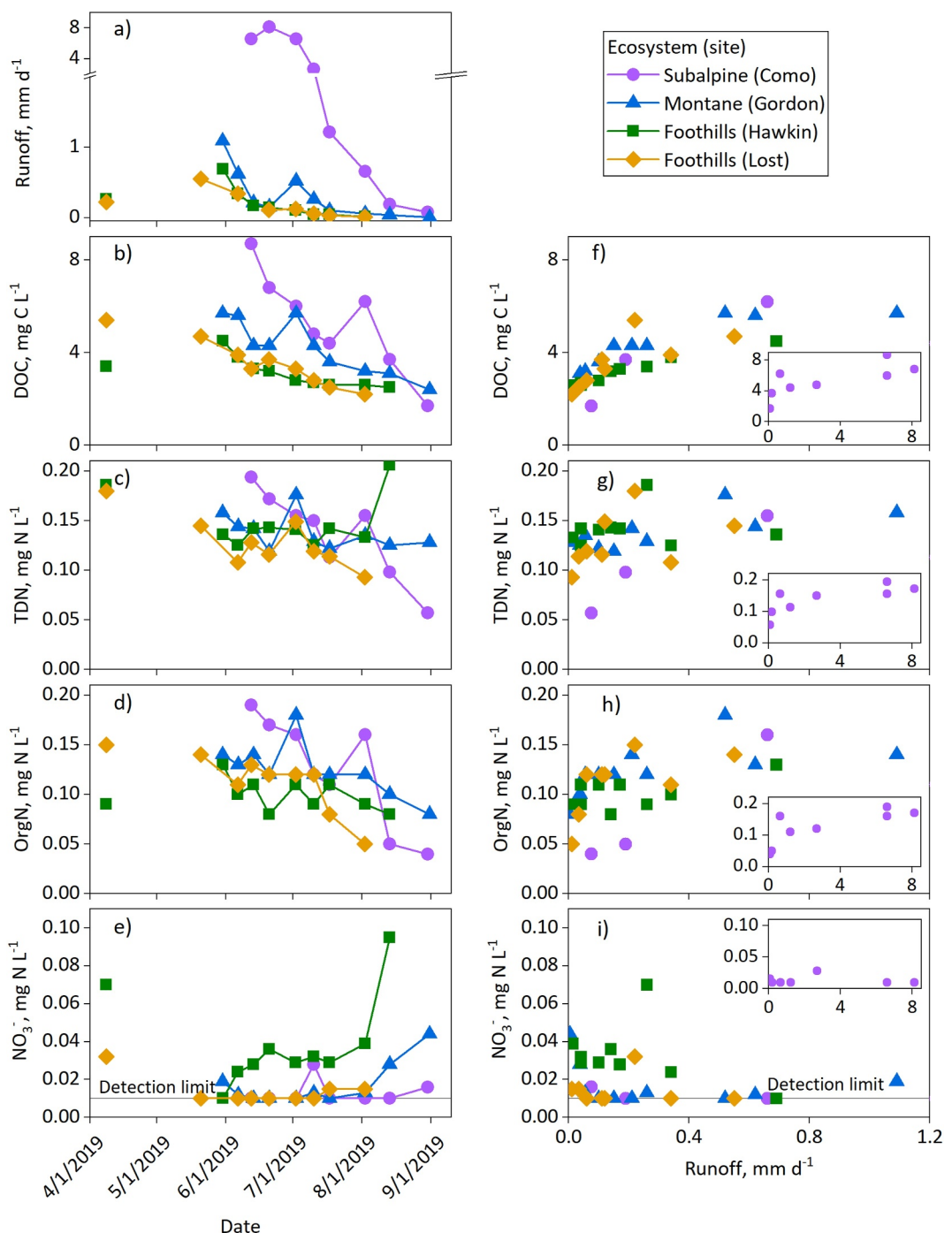


Figure 8. Surface water data collected from study watersheds, showing (a) runoff, in millimeters per day, (b) total dissolved nitrogen (TDN), in milligrams (mg) nitrogen (N) per liter (L), (c) dissolved organic carbon (DOC), in mg carbon (C) per L, (d) organic nitrogen (OrgN), in mg N per L, and (e) nitrate (NO_3^-), in mg N per L. The relationships of runoff to stream concentrations of nitrogen and carbon are shown in (f)–(i). The subalpine site (Como) relationships are shown in the inset of plots (f)–(i).

Subalpine site are associated with low soil pH and high rates of organic matter input from the subalpine vegetation (Chen et al., 2020; Clow & Sueker, 2000).

Given the gradients in soil characteristics and atmospheric N deposition, we anticipated distinct microbial communities in the soils along the elevation transect. However, we found that while microbial communities were distinct at the Subalpine site, the communities at the other three sites were very similar. The low soil pH, high C:N

ratio, and potentially anoxic conditions of the Subalpine site soil are likely responsible for the larger proportion of Acidobacteriota, which are known to thrive in acidic environments, and the very small proportion of the known ammonia oxidizers *Nitrososphaeraceae* found at that site (Figure 5). While the majority of soil microbial community research conducted in the Colorado Front Range has focused on the alpine zone (e.g., Lipson et al., 2002; Williams et al., 2007), the community composition we observed at the Montane site aligns with other previous research at this site, which found similar dominant taxa in surface soils (Eilers et al., 2012; Gabor et al., 2014). It is important to note that while the microbial communities did not differ significantly across the three lower elevation sites, the total microbial biomass was generally less at the Montane site compared to the other sites (see Repert et al., 2023), which may have important implications for N transformations. Indeed, a recent comprehensive review found that soil microbial biomass was the main driver controlling N transformation rates and thus N availability (Li et al., 2019).

Rates of N transformations varied significantly across the elevation transect but did not follow the systematic pattern we anticipated, or the microbial community composition differences described above. At the Subalpine site, the low proportion of ammonia oxidizers (*Nitrososphaeraceae*) (Figure 5) corresponded with a low abundance of *amoA*, the gene responsible for ammonia oxidation, as well as low net nitrification and nitrification potential rates. This trend is likely attributable to the lower pH levels at this site, which may inhibit the oxidation of NH_4^+ through nitrification. This Subalpine site has previously been found to have negative net N mineralization during the growing season (Chen et al., 2020). Interestingly, the Foothills site also had a low abundance of *amoA* and low net nitrification and mineralization rates, even though the proportion of ammonia oxidizers did not differ from the microbial communities at the Plains and Montane sites. Nitrification potential rates at the Foothills site, however, were equivalent to those at the Montane site, suggesting that the microbial population at the Foothills site has the capacity to oxidize ammonia, but was allocating more N toward microbial growth, especially during the winter and summer seasons. The lack of nitrification in the subalpine and the microbial immobilization of N in the foothills make these ecosystems potentially important in the retention of atmospherically deposited N.

The vegetation and soil composition at the four sites in this study very likely played a role in the variability in N cycling rates. Certain species of trees and grasses have been shown to influence soil N cycling activity by competing with microorganisms for NO_3^- and NH_4^+ (Chen et al., 2024; Meister et al., 2023) or by inhibition of biological nitrification through the production of root exudates (e.g., monoterpenes, brachialactone) that block enzymes responsible for the oxidation of NH_3 to NO_3^- by AOA and AOB (Nardi et al., 2020; Subbarao et al., 2009, 2012; Ward et al., 1997). Recently, Lafitte et al. (2020) demonstrated that spruce and Nordmann fir (*Abies nordmanniana* Spach.) litter and soil extracts inhibited the growth of the nitrite-oxidizing bacteria (NOB), *Nitrobacter hamburgensis*. In addition, soils with high C:N (>30) often lead to net N immobilization relative to mineralization as the demand for N increases to support microbial growth (Girkin & Cooper, 2023; Stevenson & Cole, 1999; Verhagen & Laanbroek, 1991). In our study, the composition of the vegetation and soil at the Subalpine site, where evergreens dominated and the soil C:N was greater than 30, was significantly different compared to the Plains, Foothills, and Montane sites where soil C:N averaged ~12. Subtle differences in vegetation at these three sites may have also contributed to the variability in N cycling activity evident at the Foothills site, where net nitrification and N mineralization rates were near zero during the winter and summer sampling events and the nitrifying gene, *amoA*, was overall less abundant.

Our results point to an interesting difference between the plains and the foothills that warrants further investigation. At the sites we sampled, the plains soils followed our expectations, with high rates of net nitrification, N mineralization, and nitrification potential, suggesting the presence of a larger or more active nitrifying population at this site. This suggests that the reduced N deposited at this lower elevation site is quickly oxidized and may be mobilized rapidly from the soil, contributing to NO_3^- concentrations in nearby stream water. Conversely, the Foothills site, which also receives high levels of reduced N in atmospheric deposition, may retain deposited N as NH_4^+ or as microbial biomass. Previous work at the montane elevation of the Colorado Front Range has identified important hydrologic controls on the ability of soils to retain N, with greater microbial N uptake on north-facing slopes where there is sufficient contact time for N to be retained in organic pools (Hinckley et al., 2017). Given this known spatial variability (Hinckley et al., 2014, 2017), the differences we observed between the Plains W and Foothills sites may be due to smaller-scale variability in hydrologic flow paths and microbial biomass, rather than a consistent pattern across the elevation transect. Regardless of the scale, however, our results suggest that there is significant spatial variability across the lower elevations of the Colorado Front Range in the ability of soils to

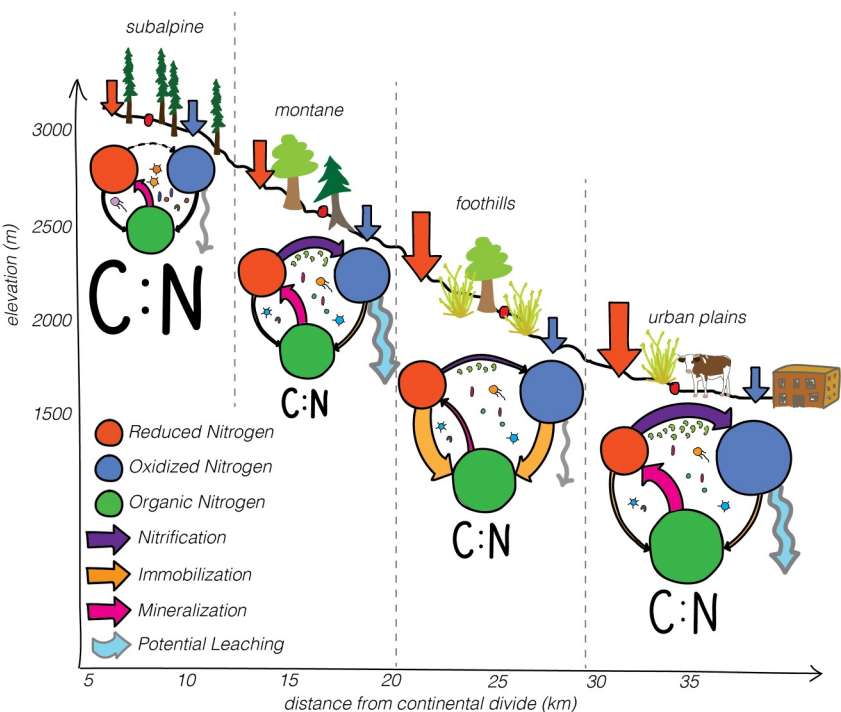


Figure 9. Schematic based on the results of this study, showing the nitrogen (N) processes, microbial community structure, and atmospheric deposition of reduced nitrogen (ammonium) and oxidized nitrogen (nitrate and nitrite) measured at study sites from the subalpine to plains. The size of the arrows and circles indicate the relative contributions of the N cycling processes and N pools, respectively, found at each site.

transform and retain atmospherically deposited reduced N, even when soil properties and microbial communities are similar (Figure 9).

While atmospheric deposition follows a clear seasonal pattern, with highest deposition rates during the spring months, rates of soil N transformations and the soil microbial community composition did not follow a consistent seasonal pattern. This lack of seasonal variability in the soil microbial community composition contrasts with previous work from the alpine zone, where soil microbial biomass and community structure follow clear seasonal patterns driven by the extreme swings in temperature and snowmelt (Lipson et al., 2002; Lipson & Schmidt, 2004; Nemergut et al., 2005). Instead of seasonal variability, the greatest temporal variability we observed was between the two fall seasons that we sampled, ON 2018 and SO 2019 (Figure 4). In ON 2018, the montane soils had unusually high concentrations of extractable nutrients and high rates of net nitrification and N mineralization, while the plains soils had unusually low concentrations of extractable nutrients and low rates of N transformations. On the other hand, SO 2019 was more similar to the other seasons, with the plains having higher concentrations of extractable nutrients and rates of N transformations compared to the montane. Although we are unable to say definitely what drove this interannual variability, 2018 was a drier year in the Colorado Front Range compared to 2019 (Heindel et al., 2022), and antecedent soil moisture is an important control on N transformation rates (Chen et al., 2020; Hinckley et al., 2017). This interannual variability is another area for further investigation, given the increasing potential for extreme weather events and extended drought conditions in the western U.S. (Zhang et al., 2021).

4.2. Current and Future Implications for Water Quality

Currently, export of NO_3^- to streams is low in the montane and foothills watersheds analyzed here. Levels of N deposition in these watersheds ($\sim 5 \text{ kg N per hectare per year}$) are below a threshold level of roughly $5\text{--}15 \text{ kg N per hectare per year}$ that leads to leaching of NO_3^- to streams in forested ecosystems (Lassiter et al., 2023; Lin et al., 2024). The lack of recent changes in stream NO_3^- in the western region of the U.S. has been attributed to these relatively lower loads of N deposition compared to the eastern U.S., where changes are much more apparent

and can be more clearly tied to reductions in N deposition in recent decades (Lin et al., 2024). However, if this region were to see increased levels of nitrogen deposition above 5–15 kg N per hectare per year in the future, it could potentially lead to leaching of nitrate and increased concentrations in nearby surface waters. In addition, it is important to note that the atmospheric deposition of 4–5 kg N per hectare per year may still be above the critical load for this region; significant ecological consequences of chronic N deposition have been well documented in the Colorado Front Range (e.g., Baron et al., 2000).

The ability of soils to process and retain N deposition at the mid-elevations of the Colorado Front Range may contrast with soils at the highest and lowest elevations of the elevation transect. In the alpine zone, persistently high stream water NO_3^- concentrations may be the result of microbially processed atmospheric reduced N deposition (Clark et al., 2021). In this ecosystem, thin soils, steep slopes, and limited vegetation may limit the ability of the terrestrial environment to retain N, enhancing the impact of atmospheric N deposition on water quality (Clow & Sueker, 2000; Mast et al., 2011, 2014). Indeed, in the Loch Vale watershed in Rocky Mountain National Park, the critical load was hindcast to be 1.5 kg N per hectare per year, well below the current rates of deposition in the alpine zone (Baron, 2006). At the lowest elevation plains ecosystems, less is known about the direct impact of N deposition on water quality, given the confounding inputs from other sources, such as fertilizer runoff and wastewater discharge. A recent modeling paper attributes 25%–44% of the estimated South Platte River total N load at the Denver gage to atmospheric deposition, one-third of which was attributed to urban deposition, suggesting that there is a significant impact of atmospheric deposition to water quality at the lowest elevations of the elevation gradient (Wetherbee et al., 2022). However, additional monitoring and modeling efforts are needed to verify these results across the plains ecoregion.

While the current rates of N deposition and soil N retention may allow the mid-elevations of the Colorado Front Range to absorb elevated N deposition without impairing water quality, a number of factors may alter current conditions. First, this region will likely see continued increases in the deposition of reduced N, given the rapid development of the Denver metro area and agricultural intensification. While the conversion of agricultural land to suburban development has the potential to decrease agricultural ammonia emissions, vehicles are an increasingly significant source of ambient ammonia to this region (Felix et al., 2023). Second, changes to precipitation patterns—extreme precipitation events, extended drought, and changes to the balance between rain and snow—will likely impact mobilization of chemical constituents (Hinckley et al., 2014). Third, wildfire is a growing concern in the western U.S.; wildfires have the potential to not only contribute to reactive N emissions, but also to severely limit the ability of the soil to retain and process N (Heindel et al., 2022 and citations within). Several studies have observed sustained elevated NO_3^- concentrations for at least 5 years after wildfire in the Colorado Front Range (Mast et al., 2016; Murphy et al., 2015, 2018; Rhoades et al., 2019). Finally, changing land cover, from development, invasive species (Hinckley et al., 2022), or from drought and wildfire disturbances has the potential to reduce the terrestrial demand for N, allowing more to be mobilized to adjacent water bodies.

5. Conclusions

While elevation explained the variability in N deposition rates and pools of total and extractable soil N, the variability we observed in the soil microbial communities, N transformation rates, and water quality was not driven primarily by elevation. Microbial community composition was similar at the Plains, Foothills, and Montane sites, but was distinct at the Subalpine site, where we also observed a higher C:N ratio and lower pH. Microbial community composition also did not vary seasonally, suggesting that there is remarkable temporal and spatial stability in the microbial community composition at the lower elevations of the Colorado Front Range.

Even though the microbial communities were similar, we observed significant variability in soil N transformation rates, suggesting that factors other than microbial community composition and atmospheric N deposition rates are important controls on soil N cycling. Net nitrification, net N mineralization, and nitrification potential rates were highest at the Plains and Montane sites, where there was also higher abundance of the *amoA* gene, suggesting that these sites have the potential to mobilize N to adjacent water bodies. In contrast, we observed net immobilization of N at the Foothills and Subalpine sites, where more N may be allocated for microbial growth, suggesting that these sites retain atmospherically deposited N. The spatial variability in soil N cycling that we observed at the lower elevation sites may not be driven by elevation, but may exist at finer spatial scales, due to soil, vegetation, or microbial community characteristics not captured in this study. Understanding the scale of spatial variability is an

important area for continued research, especially in the foothills and plains ecosystems, where rates of N deposition are elevated and where we observed such contrasting results.

Concentrations of NO_3^- and NH_4^+ in streams draining the subalpine to the foothills were generally low, indicating that these mid-elevation soils are able to process and retain the current level of N deposition. Runoff was an important driver of TDN at the wettest, high-elevation site, but there was no relationship between runoff and TDN at the Foothills sites. Again, the contrasting and unexpected behavior at these lower-elevation ecosystems of the Colorado Front Range warrant further study. Future rates of N deposition may increase at sites located adjacent to urban and agriculture N emissions, and these sites are also especially vulnerable to disturbances such as drought, wildfire, and land-use change, which will alter the ability of the soils to process N and may mobilize more N to adjacent water bodies.

Conflict of Interest

The authors declare no conflicts of interest relevant to this study.

Data Availability Statement

Data for generating seasonal deposition rates of NH_4^+ and $\text{NO}_3^- + \text{NO}_2^-$ using the ion exchange resin columns are available in <https://doi.org/10.5066/P9XW4TM8> (Repert et al., 2021). Soil C, N, and pH data, nitrification and mineralization data used for rate calculations, and microbial community data are available in <https://doi.org/10.5066/P99JOZ7P> (Repert et al., 2023). Soil extraction and water quality data are available in <https://doi.org/10.5066/P95PGQZ2> (Repert et al., 2024). Microbial sequence data are located in the National Center for Biotechnology Information (NCBI, 2002) Sequence Read Archive (<https://www.ncbi.nlm.nih.gov/sra>) under BioProject no. PRJNA1001006 and accession numbers SAMN36786223 - SAMN36786243.

Acknowledgments

The U.S. Geological Survey Ecosystems Land Change Science Program of the Ecosystems Mission Area supported the data collection, analysis, and interpretation for this study. We thank the agencies and individuals who funded and (or) hosted the sampling sites: Boulder County Parks and Open Space, City of Boulder Open Space and Mountain Parks, Colorado Department of Public Health and Environment, National Atmospheric and Deposition Program, National Science Foundation (NSF)-funded Boulder Creek Critical Zone Observatory, Niwot Ridge Long-Term Ecological Research program, University of Colorado Boulder, and Greg Wetherbee. We also thank Isaac Bukoski, Isiah Castro, Toby Halamka, Mahalie Hill, Eve-Lyn Hinckley, Tyler Kane, Janey Le, Alex Nolan, Ariel Reed, and Jennifer Underwood for assistance with sample collection, laboratory analyses, and coding, and Deborah Martin for help with vegetation identification. This manuscript was significantly improved by the suggestions of Richard L. Smith, Gregory Wetherbee, and one anonymous reviewer. Any use of trade, firm, or product names is for descriptive purposes only and does not imply endorsement by the U.S. Government.

References

Baron, J. S. (2006). Hindcasting nitrogen deposition to determine an ecological critical load. *Ecological Applications*, 16(2), 433–439. [https://doi.org/10.1890/1051-0761\(2006\)016\[0433:HNDTDA\]2.0.CO;2](https://doi.org/10.1890/1051-0761(2006)016[0433:HNDTDA]2.0.CO;2)

Baron, J. S., Rueth, H. M., Wolfe, A. M., Nydick, K. R., Allstott, E. J., Minear, J. T., & Moraska, B. (2000). Ecosystem responses to nitrogen deposition in the Colorado Front Range. *Ecosystems*, 3(4), 352–368. <https://doi.org/10.1007/s100210000032>

Benish, S. E., Bash, J. O., Foley, K. M., Appel, K. W., Hogrefe, C., Gilliam, R., & Pouliot, G. (2022). Long-term regional trends of nitrogen and sulfur deposition in the United States from 2002 to 2017. *Atmospheric Chemistry and Physics*, 22(19), 12749–12767. <https://doi.org/10.5194/acp-22-12749-2022>

Bokulich, N. A., Kaehler, B. D., Rideout, J. R., Dillon, M., Bolyen, E., Knight, R., et al. (2018). Optimizing taxonomic classification of marker-gene amplicon sequences with QIIME 2's q2-feature-classifier plugin. *Microbiome*, 6, 1–17. <https://doi.org/10.1186/s40168-018-0470-z>

Bolyen, E., Rideout, J. R., Dillon, M. R., Bokulich, N. A., Abnet, C. C., Al-Ghalith, G. A., et al. (2019). Reproducible, interactive, scalable and extensible microbiome data science using QIIME 2. *Nature Biotechnology*, 37(8), 852–857. <https://doi.org/10.1038/s41587-019-0209-9>

Booth, M. S., Stark, J. M., & Rastetter, E. (2005). Controls on nitrogen cycling in terrestrial ecosystems: A synthetic analysis of literature data. *Ecological Monographs*, 75(2), 139–157. <https://doi.org/10.1890/04-0988>

Bowman, W. D., Ayyad, A., Bueno de Mesquita, C. P., Fierer, N., Potter, T. S., & Sternagel, S. (2018). Limited ecosystem recovery from simulated chronic nitrogen deposition. *Ecological Applications*, 28(7), 1762–1772. <https://doi.org/10.1002/eaap.1783>

Boyer, E. W., Hornberger, G. M., Bencala, K. E., & McKnight, D. M. (1997). Response characteristics of DOC flushing in an alpine catchment. *Hydrological Processes*, 11(12), 1635–1647. [https://doi.org/10.1002/\(SICI\)1099-1085\(19971015\)11:12<1635::AID-HYP494>3.0.CO;2-H](https://doi.org/10.1002/(SICI)1099-1085(19971015)11:12<1635::AID-HYP494>3.0.CO;2-H)

Brigham, L. M., Bueno de Mesquita, C. P., Smith, J. G., Sartwell, S. A., Schmidt, S. K., & Suding, K. N. (2022). Do plant–soil interactions influence how the microbial community responds to environmental change? *Ecology*, 103(1), e03554. <https://doi.org/10.1002/ecy.3554>

Bukoski, I. S., Murphy, S. F., Birch, A. L., & Barnard, H. R. (2021). Summer runoff generation in foothill catchments of the Colorado Front Range. *Journal of Hydrology*, 595, 125672. <https://doi.org/10.1016/j.jhydrol.2020.125672>

Callahan, B. J., McMurdie, P. J., Rosen, M. J., Han, A. W., Johnson, A. J. A., & Holmes, S. P. (2016). DADA2: High-resolution sample inference from Illumina amplicon data. *Nature Methods*, 13(7), 581–583. <https://doi.org/10.1038/nmeth.3869>

Caporaso, J. G., Lauber, C. L., Walters, W. A., Berg-Lyons, D., Lozupone, C. A., Turnbaugh, P. J., et al. (2011). Global patterns of 16S rRNA diversity at a depth of millions of sequences per sample. *Proceedings of the National Academy of Sciences of the United States of America*, 108(supplement 1), 4516–4522. <https://doi.org/10.1073/pnas.1000080107>

Carreiro, M. M., Sinsabaugh, R. L., Repert, D. A., & Parkhurst, D. F. (2000). Microbial enzyme shifts explain litter decay responses to simulated nitrogen deposition. *Ecology*, 81(9), 2359–2365. [https://doi.org/10.1890/0012-9658\(2000\)081\[2359:MESELD\]2.0.CO;2](https://doi.org/10.1890/0012-9658(2000)081[2359:MESELD]2.0.CO;2)

Chen, J., Li, F. C., Jia, B., Gang, S., Li, Y., Mou, X. M., et al. (2024). Regulation of soil nitrogen cycling by shrubs in grasslands. *Soil Biology and Biochemistry*, 191, 109327. <https://doi.org/10.1016/j.soilbio.2024.109327>

Chen, Y., Wieder, W. R., Hermes, A. L., & Hinckley, E. L. S. (2020). The role of physical properties in controlling soil nitrogen cycling across a tundra-forest ecotone of the Colorado Rocky Mountains, USA. *Catena*, 186, 104369. <https://doi.org/10.1016/j.catena.2019.104369>

Clark, S. C., Barnes, R. T., Oleksy, I. A., Baron, J. S., & Hastings, M. G. (2021). Persistent nitrate in alpine waters with changing atmospheric deposition and warming trends. *Environmental Science & Technology*, 55(21), 14946–14956. <https://doi.org/10.1021/acs.est.1c02515>

Clow, D. W., & Sueker, J. K. (2000). Relations between basin characteristics and stream water chemistry in alpine/subalpine basins in Rocky Mountain National Park, Colorado. *Water Resources Research*, 36(1), 49–61. <https://doi.org/10.1029/1999WR900294>

Cole, J. C., & Braddock, W. A. (2009). *Geologic map of the Estes Park 30' X 60' Quadrangle, North-central Colorado* (p. 56). U.S. Department of the Interior, U.S. Geological Survey. Retrieved from <https://pubsdata.usgs.gov/pubs/sim/3039/index.html>

Crowther, T. W., Van den Hoogen, J., Wan, J., Mayes, M. A., Keiser, A. D., Mo, L., et al. (2019). The global soil community and its influence on biogeochemistry. *Science*, 365(6455), eaav0550. <https://doi.org/10.1126/science.aav0550>

Daims, H., Lebedeva, E. V., Pjevac, P., Han, P., Herbold, C., Albertsen, M., et al. (2015). Complete nitrification by Nitrospira bacteria. *Nature*, 528(7583), 504–509. <https://doi.org/10.1038/nature16461>

Dewitz, J., & U.S. Geological Survey (2021). National land cover database (NLCD) 2019 products (ver. 2.0, June 2021) [Dataset]. U.S. Geological Survey data release. <https://doi.org/10.5066/P9KZCM54>

Driscoll, C., Milford, J. B., Henze, D. K., & Bell, M. D. (2024). Atmospheric reduced nitrogen: Sources, transformations, effects, and management. *Journal of the Air & Waste Management Association*, 74(6), 362–415. <https://doi.org/10.1080/10962247.2024.2342765>

Du, E., de Vries, W., Galloway, J. N., Hu, X., & Fang, J. (2014). Changes in wet nitrogen deposition in the United States between 1985 and 2012. *Environmental Research Letters*, 9(9), 095004. <https://doi.org/10.1088/1748-9326/9/9/095004>

Eilers, K. G., Debenport, S., Anderson, S., & Fierer, N. (2012). Digging deeper to find unique microbial communities: The strong effect of depth on the structure of bacterial and archaeal communities in soil. *Soil Biology and Biochemistry*, 50, 58–65. <https://doi.org/10.1016/j.soilbio.2012.03.011>

Felix, J. D., Berner, A., Wetherbee, G. A., Murphy, S. F., & Heindel, R. C. (2023). Nitrogen isotopes indicate vehicle emissions and biomass burning dominate ambient ammonia across Colorado's Front Range urban corridor. *Environmental Pollution*, 316, 120537. <https://doi.org/10.1016/j.envpol.2022.120537>

Fenn, M. E., Bytnerowicz, A., Schilling, S. L., Vallano, D. M., Zavaleta, E. S., Weiss, S. B., et al. (2018). On-road emissions of ammonia: An underappreciated source of atmospheric nitrogen deposition. *Science of the Total Environment*, 625, 909–919. <https://doi.org/10.1016/j.scitotenv.2017.12.313>

Fierer, N., Lauber, C. L., Ramirez, K. S., Zaneveld, J., Bradford, M. A., & Knight, R. (2012). Comparative metagenomic, phylogenetic and physiological analyses of soil microbial communities across nitrogen gradients. *The ISME Journal*, 6(5), 1007–1017. <https://doi.org/10.1038/ismej.2011.159>

Fog, K. (1988). The effect of added nitrogen on the rate of decomposition of organic matter. *Biological Reviews*, 63(3), 433–462. <https://doi.org/10.1111/j.1469-185X.1988.tb00725.x>

Freedman, Z. B., Romanowicz, K. J., Upchurch, R. A., & Zak, D. R. (2015). Differential responses of total and active soil microbial communities to long-term experimental N deposition. *Soil Biology and Biochemistry*, 90, 275–282. <https://doi.org/10.1016/j.soilbio.2015.08.014>

Gabor, R. S., Eilers, K., McKnight, D. M., Fierer, N., & Anderson, S. P. (2014). From the litter layer to the saprolite: Chemical changes in water-soluble soil organic matter and their correlation to microbial community composition. *Soil Biology and Biochemistry*, 68, 166–176. <https://doi.org/10.1016/j.soilbio.2013.09.029>

Garside, C. (1982). A chemiluminescent technique for the determination of nanomolar concentrations of nitrate and nitrite in seawater. *Marine Chemistry*, 11(2), 159–167. [https://doi.org/10.1016/0304-4203\(82\)90039-1](https://doi.org/10.1016/0304-4203(82)90039-1)

Girkin, N. T., & Cooper, H. V. (2023). Nitrogen and ammonia in soils. In *Module in Earth systems and environmental sciences*. Elsevier. <https://doi.org/10.1016/B978-0-12-822974-3.00010-0>

Hart, S. C., Stark, J. M., Davidson, E. A., & Firestone, M. K. (1994). Nitrogen mineralization, immobilization, and nitrification. *Methods of Soil Analysis: Part 2 Microbiological and Biochemical Properties*, 5, 985–1018. <https://doi.org/10.2136/sssabookser5.2.c42>

Heindel, R. C., Murphy, S. F., Repert, D. A., Wetherbee, G. A., Liethen, A. E., Clow, D. W., & Halamka, T. A. (2022). Elevated nitrogen deposition to fire-prone forests adjacent to urban and agricultural areas, Colorado Front Range, USA. *Earth's Future*, 10(7). <https://doi.org/10.1029/2021EF002373>

Hinckley, E. L. S., Ebel, B. A., Barnes, R. T., Anderson, R. S., Williams, M. W., & Anderson, S. P. (2014). Aspect control of water movement on hillslopes near the rain–snow transition of the Colorado Front Range. *Hydrological Processes*, 28(1), 74–85. <https://doi.org/10.1002/hyp.9549>

Hinckley, E. L. S., Ebel, B. A., Barnes, R. T., Murphy, S. F., & Anderson, S. P. (2017). Critical zone properties control the fate of nitrogen during experimental rainfall in montane forests of the Colorado Front Range. *Biogeochemistry*, 132(1–2), 213–231. <https://doi.org/10.1007/s10533-017-0299-8>

Hinckley, E. L. S., Miller, H. R., Lezberg, A., & Anacker, B. (2022). Interactions between tall oatgrass invasion and soil nitrogen cycling. *Oecologia*, 199(2), 419–426. <https://doi.org/10.1007/s00442-022-05192-x>

Homyak, P. M., Vasquez, K. T., Sickman, J. O., Parker, D. R., & Schimel, J. P. (2015). Improving nitrite analysis in soils: Drawbacks of the conventional 2 M KCl extraction. *Soil Science Society of America Journal*, 79(4), 1237–1242. <https://doi.org/10.2136/sssaj2015.02.0061n>

Katoh, K., Misawa, K., Kuma, K.-I., & Miyata, T. (2002). MAFFT: A novel method for rapid multiple sequence alignment based on fast Fourier transform. *Nucleic Acids Research*, 30(14), 3059–3066. <https://doi.org/10.1093/nar/gkf436>

Kellogg, K. S., Shroba, R. R., Bryant, B., & Premo, W. R. (2008). Geologic map of the Denver west 30' × 60' quadrangle, north-central Colorado. In *U.S. geological survey scientific investigations map 3000*. Retrieved from <https://pubsdata.usgs.gov/pubs/sim/3000/index.html>

Kozich, J. J., Westcott, S. L., Baxter, N. T., Highlander, S. K., & Schloss, P. D. (2013). Development of a dual-index sequencing strategy and curation pipeline for analyzing amplicon sequence data on the MiSeq Illumina sequencing platform. *Applied and Environmental Microbiology*, 79(17), 5112–5120. <https://doi.org/10.1128/AEM.01043-13>

Laffite, A., Florio, A., Andrianarisoa, K. S., Creuze des Chatelliers, C., Schlüter-Hai, B., Ndaw, S. M., et al. (2020). Biological inhibition of soil nitrification by forest tree species affects Nitrobacter populations. *Environmental Microbiology*, 22(3), 1141–1153. <https://doi.org/10.1111/1462-2920.14905>

Lassiter, M. G., Lin, J., Compton, J. E., Phelan, J., Sabo, R. D., Stoddard, J. L., et al. (2023). Shifts in the composition of nitrogen deposition in the conterminous United States are discernible in stream chemistry. *Science of the Total Environment*, 881, 163409. <https://doi.org/10.1111/1462-2920.14905>

Li, J., Sang, C., Yang, J., Qu, L., Xia, Z., Sun, H., et al. (2021). Stoichiometric imbalance and microbial community regulate microbial elements use efficiencies under nitrogen addition. *Soil Biology and Biochemistry*, 156, 108207. <https://doi.org/10.1016/j.soilbio.2021.108207>

Li, K. Y., Zhao, Y. Y., Yuan, X. L., Zhao, H. B., Wang, Z. H., Li, S. X., & Malhi, S. S. (2012). Comparison of factors affecting soil nitrate nitrogen and ammonium nitrogen extraction. *Communications in Soil Science and Plant Analysis*, 43(3), 571–588. <https://doi.org/10.1080/00103624.2012.639108>

Li, Y., Schichtel, B. A., Walker, J. T., Schwede, D. B., Chen, X., Lehmann, C. M., et al. (2016). Increasing importance of deposition of reduced nitrogen in the United States. *Proceedings of the National Academy of Sciences of the United States of America*, 113(21), 5874–5879. <https://doi.org/10.1073/pnas.1525736113>

Li, Z., Tian, D., Wang, B., Wang, J., Wang, S., Chen, H. Y., et al. (2019). Microbes drive global soil nitrogen mineralization and availability. *Global Change Biology*, 25(3), 1078–1088. <https://doi.org/10.1111/gcb.14557>

Lieb, A. M., Darrouzet-Nardi, A., & Bowman, W. D. (2011). Nitrogen deposition decreases acid buffering capacity of alpine soils in the southern Rocky Mountains. *Geoderma*, 164(3–4), 220–224. <https://doi.org/10.1016/j.geoderma.2011.06.013>

Likens, G. E., Butler, T. J., Claybrooke, R., Vermeylen, F., & Larson, R. (2021). Long-term monitoring of precipitation chemistry in the U.S.: Insights into changes and condition. *Atmospheric Environment*, 245, 118031. <https://doi.org/10.1016/j.atmosenv.2020.118031>

Lin, J., Compton, J. E., Sabo, R. D., Herlihy, A. T., Hill, R. A., Weber, M. H., et al. (2024). The changing nitrogen landscape of United States streams: Declining deposition and increasing organic nitrogen. *PNAS Nexus*, 3(1), pgad362. <https://doi.org/10.1093/pnasnexus/pgad362>

Lindaas, J., Pollack, I. B., Garofalo, L. A., Pothier, M. A., Farmer, D. K., Kreidenweis, S. M., et al. (2021). Emissions of reactive nitrogen from western U.S. wildfires during Summer 2018. *Journal of Geophysical Research: Atmospheres*, 126(2), e2020JD032657. <https://doi.org/10.1029/2020JD032657>

Lipson, D. A., Schadt, C. W., & Schmidt, S. K. (2002). Changes in soil microbial community structure and function in an alpine dry meadow following spring snow melt. *Microbial Ecology*, 43(3), 307–314. <https://doi.org/10.1007/s00248-001-1057-x>

Lipson, D. A., & Schmidt, S. K. (2004). Seasonal changes in an alpine soil bacterial community in the Colorado Rocky Mountains. *Applied and Environmental Microbiology*, 70(5), 2867–2879. <https://doi.org/10.1128/AEM.70.5.2867-2879.2004>

Lozupone, C., & Knight, R. (2005). UniFrac: A new phylogenetic method for comparing microbial communities. *Applied and Environmental Microbiology*, 71(12), 8228–8235. <https://doi.org/10.1128/AEM.71.12.8228-8235.2005>

Lozupone, C. A., Hamady, M., Kelley, S. T., & Knight, R. (2007). Quantitative and qualitative β diversity measures lead to different insights into factors that structure microbial communities. *Applied and Environmental Microbiology*, 73(5), 1576–1585. <https://doi.org/10.1128/AEM.01996-06>

Mast, M. A., Clow, D. W., Baron, J. S., & Wetherbee, G. A. (2014). Links between N deposition and nitrate export from a high-elevation watershed in the Colorado Front Range. *Environmental Science & Technology*, 48(24), 14258–14265. <https://doi.org/10.1021/es502461k>

Mast, M. A., Murphy, S. F., Clow, D. W., Penn, C. A., & Sextone, G. A. (2016). Water-quality response to a high-elevation wildfire in the Colorado Front Range. *Hydrological Processes*, 30(12), 1811–1823. <https://doi.org/10.1002/hyp.10755>

Mast, M. A., Turk, J. T., Clow, D. W., & Campbell, D. H. (2011). Response of lake chemistry to changes in atmospheric deposition and climate in three high-elevation wilderness areas of Colorado. *Biogeochemistry*, 103(1–3), 27–43. <https://doi.org/10.1007/s10533-010-9443-4>

McCleskey, R. B., Writer, J. H., & Murphy, S. F. (2012). Water chemistry data for surface waters impacted by the Fourmile Canyon Wildfire, Colorado, 2010–2011. U.S. Geological Survey Open-File Report. 2012–1104. U.S. Geological Survey. <https://doi.org/10.3133/of20121104>

Meister, A., Bohm, K., Gutiérrez-Ginés, M. J., Gaw, S., Dickinson, N., & Robinson, B. (2023). Effects of native plants on nitrogen cycling microorganisms in soil. *Applied Soil Ecology*, 191, 105031. <https://doi.org/10.1016/j.apsoil.2023.105031>

Murphy, S. F. (2006). State of the watershed: Water quality of Boulder Creek, Colorado: U.S. Geological Survey Circular. 1284 (p. 34). <https://doi.org/10.3133/circ1284>

Murphy, S. F., McCleskey, R. B., Martin, D. A., Writer, J. H., & Ebel, B. A. (2018). Fire, flood, and drought: Extreme climate events alter flow paths and stream chemistry. *Journal of Geophysical Research: Biogeosciences*, 123(8), 2513–2526. <https://doi.org/10.1029/2017JG004349>

Murphy, S. F., Writer, J. H., McCleskey, R. B., & Martin, D. A. (2015). The role of precipitation type, intensity, and spatial distribution in source water quality after wildfire. *Environmental Research Letters*, 10(8), 084007. <https://doi.org/10.1088/1748-9326/10/8/084007>

Nardi, P., Laanbroek, H. J., Nicol, G. W., Renella, G., Cardinale, M., Pietramallara, G., et al. (2020). Biological nitrification inhibition in the rhizosphere: Determining interactions and impact on microbially mediated processes and potential applications. *FEMS Microbiology Reviews*, 44(6), 874–908. <https://doi.org/10.1093/femsre/fuaa037>

National Atmospheric Deposition Program. (2022). NTN site information. Retrieved from <https://nadp.slu.wisc.edu/maps-data/ntn-interactive-map/>

National Center for Biotechnology Information. (2002). The NCBI handbook [Internet] [Dataset]. Bethesda (MD): National Library of Medicine (US). *National Center for Biotechnology Information*. Retrieved from <http://www.ncbi.nlm.nih.gov/books/NBK21101>

Nemergut, D. R., Costello, E. K., Meyer, A. F., Pescador, M. Y., Weintraub, M. N., & Schmidt, S. K. (2005). Structure and function of alpine and arctic soil microbial communities. *Research in Microbiology*, 156(7), 775–784. <https://doi.org/10.1016/j.resmic.2005.03.004>

Oksanen, J., Simpson, G. L., Blanchet, F. G., Kindt, R., Legendre, P., Minchin, P. R., et al. (2024). Community ecology package [Software]. *R Package Version*, 2, 6–6.1. <https://github.com/vegadevs/vegan>

Philippot, L., Spor, A., Hénault, C., Bru, D., Bizouard, F., Jones, C. M., et al. (2013). Loss in microbial diversity affects nitrogen cycling in soil. *The ISME Journal*, 7(8), 1609–1619. <https://doi.org/10.1038/ismej.2013.34>

Potter, B. B., & Wimsatt, J. C. (2005). Method 415.3. Measurement of total organic carbon, dissolved organic carbon and specific UV absorbance at 254 nm in source water and drinking water. US Environmental protection agency. <https://doi.org/10.5942/jawwa.2012.104.0086>

Price, M. N., Dehal, P. S., & Arkin, A. P. (2010). FastTree 2—approximately maximum-likelihood trees for large alignments. *PLoS One*, 5(3), e9490. <https://doi.org/10.1371/journal.pone.0009490>

Pruesse, E., Quast, C., Knittel, K., Fuchs, B. M., Ludwig, W., Peplies, J., & Glöckner, F. O. (2007). SILVA: A comprehensive online resource for quality checked and aligned ribosomal RNA sequence data compatible with ARB. *Nucleic Acids Research*, 35(21), 7188–7196. <https://doi.org/10.1093/nar/gkm864>

Quast, C., Pruesse, E., Yilmaz, P., Gerken, J., Schweer, T., Yarza, P., et al. (2012). The SILVA ribosomal RNA gene database project: Improved data processing and web-based tools. *Nucleic Acids Research*, 41(D1), D590–D596. <https://doi.org/10.1093/nar/gks1219>

R Core Team. (2024). R: A language and environment for statistical computing [Software]. *R Foundation for Statistical Computing*. Retrieved from <https://www.r-project.org/>

Repert, D. A., Halamka, T. A., Jeanis, K. M., & Murphy, S. F. (2023). Biological N-cycling data from soils collected along an elevation gradient in the CO Front Range (2018–2019) (ver. 2.0, November 2024) [Dataset]. U.S. Geological Survey data release. <https://doi.org/10.5066/P991OZ7P>

Repert, D. A., Murphy, S. F., Halamka, T. A., Hill, M. M., Heindel, R. C., & Clow, D. W. (2021). Seasonal atmospheric nitrate and ammonium deposition along an elevation gradient in the Colorado Front Range using ion exchange resin columns (2018–2019) [Dataset]. U.S. Geological Survey data release. <https://doi.org/10.5066/P9XW4TM8>

Repert, D. A., Tomaszewski, E. J., Marquez, J. A., Castro, I. R., McCleskey, R. B., Roth, D. A., et al. (2024). Biogeochemical data from field samples and laboratory experiments, Boulder Creek Watershed, Colorado (2019–2023) [Dataset]. U.S. Geological Survey data release. <https://doi.org/10.5066/P95PGQZ2>

Repert, D. A., Underwood, J. C., Smith, R. L., & Song, B. (2014). Seasonal nitrogen cycling processes and relationship to microbial community structure in bed sediments from the Yukon River at Pilot Station. *Journal of Geophysical Research: Biogeoscience*, 119(12), 2328–2344. <https://doi.org/10.1002/2014JG002707>

Revelle, W. (2024). Procedures for psychological, psychometric, and personality research [Software]. *R Package Version* 2.4.6.26. <https://personality-project.org/r/psych>

Rhoades, C. C., Chow, A. T., Covino, T. P., Fegel, T. S., Pierson, D. N., & Rhea, A. E. (2019). The legacy of a severe wildfire on stream nitrogen and carbon in headwater catchments. *Ecosystems*, 22(3), 643–657. <https://doi.org/10.1007/s10021-018-0293-6>

Robeson, M. S., O'Rourke, D. R., Kaehler, B. D., Ziemska, M., Dillon, M. R., Foster, J. T., & Bokulich, N. A. (2021). RESCRIPt: Reproducible sequence taxonomy reference database management. *PLoS Computational Biology*, 17(11), e1009581. <https://doi.org/10.1371/journal.pcbi.1009581>

Rognes, T., Flouri, T., Nichols, B., Quince, C., & Mahé, F. (2016). VSEARCH: A versatile open source tool for metagenomics. *PeerJ*, 4, e2584. <https://doi.org/10.7717/peerj.2584>

Rotthauwe, J. H., Witzel, K. P., & Liesack, W. (1997). The ammonia monooxygenase structural gene *amoA* as a functional marker: Molecular fine-scale analysis of natural ammonia-oxidizing populations. *Applied and Environmental Microbiology*, 63(12), 4704–4712. <https://doi.org/10.1128/aem.63.12.4704-4712.1997>

Scheiner, D. (1976). Determination of ammonia and Kjeldahl nitrogen by indophenol method. *Water Research*, 10(1), 31–36. [https://doi.org/10.1016/0043-1354\(76\)90154-8](https://doi.org/10.1016/0043-1354(76)90154-8)

Smith, R. L., Repert, D. A., Barber, L. B., & LeBlanc, D. R. (2013). Long-term groundwater contamination after source removal—The role of sorbed carbon and nitrogen on the rate of reoxygenation of a treated-wastewater plume on Cape Cod, MA, USA. *Chemical Geology*, 337, 38–47. <https://doi.org/10.1016/j.chemgeo.2012.11.007>

Smith, R. L., Repert, D. A., Stoliker, D. L., Kent, D. B., Song, B., LeBlanc, D. R., et al. (2019). Seasonal and spatial variation in the location and reactivity of a nitrate-contaminated groundwater discharge zone in a lakebed. *Journal of Geophysical Research: Biogeosciences*, 124(7), 2186–2207. <https://doi.org/10.1029/2018jg004635>

Stevenson, F. J., & Cole, M. A. (1999). *Cycles of soils: Carbon, nitrogen, phosphorus, sulfur, micronutrients*. John Wiley & Sons.

Subbarao, G. V., Nakahara, K., Hurtado, M. D. P., Ono, H., Moreta, D. E., Salcedo, A. F., et al. (2009). Evidence for biological nitrification inhibition in Brachiaria pastures. *Proceedings of the National Academy of Sciences of the United States of America*, 106(41), 17302–17307. <https://doi.org/10.1073/pnas.0903694106>

Subbarao, G. V., Sahrawat, K. L., Nakahara, K., Ishikawa, T., Kishii, M., Rao, I. M., et al. (2012). Biological nitrification inhibition—A novel strategy to regulate nitrification in agricultural systems. *Advances in Agronomy*, 114, 249–302. <https://doi.org/10.1016/B978-0-12-394275-3.00001-8>

U.S. Geological Survey. (2019). The StreamStats program. Retrieved from <https://streamstats.usgs.gov/ss/>

Van Kessel, M. A., Speth, D. R., Albertsen, M., Nielsen, P. H., Op den Camp, H. J., Kartal, B., et al. (2015). Complete nitrification by a single microorganism. *Nature*, 528(7583), 555–559. <https://doi.org/10.1038/nature16459>

Verhagen, F. J., & Laanbroek, H. J. (1991). Competition for ammonium between nitrifying and heterotrophic bacteria in dual energy-limited chemostats. *Applied and Environmental Microbiology*, 57(11), 3255–3263. <https://doi.org/10.1128/aem.57.11.3255-3263.1991>

Ward, B. B., Courtney, K. J., & Langenheim, J. H. (1997). Inhibition of *Nitrosomonas europaea* by monoterpenes from coastal redwood (*Sequoia sempervirens*) in whole-cell studies. *Journal of Chemical Ecology*, 23(11), 2583–2598. <https://doi.org/10.1023/B:JOEC.000000668.48855.b7>

Westerling, A. L., Hidalgo, H. G., Cayan, D. R., & Swetnam, T. W. (2006). Warming and earlier spring increase western U.S. forest wildfire activity. *Science*, 313(5789), 940–943. <https://doi.org/10.1126/science.1128834>

Wetherbee, G., Wieczorek, M., Robertson, D., Saad, D., Novick, J., & Mast, M. A. (2022). Estimating urban air pollution contribution to South Platte River nitrogen loads with National Atmospheric Deposition Program data and SPARROW model. *Journal of Environmental Management*, 301, 113861. <https://doi.org/10.1016/j.jenvman.2021.113861>

Wetherbee, G. A., Benedict, K. B., Murphy, S. F., & Elliott, E. M. (2019). Inorganic nitrogen wet deposition gradients in the Denver-Boulder metropolitan area and Colorado Front Range—Preliminary implications for Rocky Mountain National Park and interpolated deposition maps. *Science of the Total Environment*, 691, 1027–1042. <https://doi.org/10.1016/j.scitotenv.2019.06.528>

Wetherbee, G. A., Murphy, S. F., Repert, D. A., Heindel, R. C., & Liethen, E. A. (2021). Chemical analyses and precipitation depth data for wet deposition samples collected as part of the National Atmospheric Deposition Program in the Colorado Front Range, 2017–2019. *U.S. Geological Survey data release*. <https://doi.org/10.5066/P900IQ0E>

Williams, M. W., Barnes, R. T., Parman, J. N., Freppaz, M., & Hood, E. (2011). Stream water chemistry along an elevational gradient from the Continental Divide to the foothills of the Rocky Mountains. *Vadose Zone Journal*, 10(3), 900–914. <https://doi.org/10.2136/vzj2010.0131>

Williams, M. W., Knauf, M., Cory, R., Caine, N., & Liu, F. (2007). Nitrate content and potential microbial signature of rock glacier outflow, Colorado Front Range. *Earth Surface Processes and Landforms: The Journal of the British Geomorphological Research Group*, 32(7), 1032–1047. <https://doi.org/10.1002/esp.1455>

Zhang, F., Biederman, J. A., Dannenberg, M. P., Yan, D., Reed, S. C., & Smith, W. K. (2021). Five decades of observed daily precipitation reveal longer and more variable drought events across much of the western United States. *Geophysical Research Letters*, 48(7), e2020GL092293. <https://doi.org/10.1029/2020GL092293>

Zhang, T. A., Chen, H. Y., & Ruan, H. (2018). Global negative effects of nitrogen deposition on soil microbes. *The ISME Journal*, 12(7), 1817–1825. <https://doi.org/10.1038/s41396-018-0096-y>

References From the Supporting Information

Boulder County Parks and Open Space. (2009). Betasso preserve management plan including the Benjamin property. Retrieved from <https://assets.bouldercounty.gov/wp-content/uploads/2017/03/betasso-preserve-management-plan.pdf>

Humphries, H. (1993). *Plant species list for Niwot Ridge/Green Lakes Valley, 1970 - Ongoing* (Vol. 91.4). LTER Network Member Node. knb-lter-nwt.

Korb, J. E., & Ranker, T. A. (2001). Changes in stand composition and structure between 1981 and 1996 in four Front Range plant communities in Colorado. *Plant Ecology*, 157(1), 1–11. <https://doi.org/10.1023/A:101377220131>

Sproull, G. J., Quigley, M. F., Sher, A., & González, E. (2015). Long-term changes in composition, diversity and distribution patterns in four herbaceous plant communities along an elevational gradient. *Journal of Vegetation Science*, 26(3), 552–563. <https://doi.org/10.1111/jvs.12264>

United States Department of Agriculture. (2024). Plants database. Retrieved from <https://plants.usda.gov/home>. accessed 8 Sept 2024.

University of Colorado Mountain Research Station. (2024). Plant species composition Niwot Ridge and Green Lakes Valley. Retrieved from <https://www.colorado.edu/mrs/research-natural-history/species-lists/plant-species-composition>. accessed 8 Sept 2024.